RM E55J13a

NACA

# RESEARCH MEMORANDUM

## INTERFERENCE EFFECTS AT MACH 1.9 ON A HORIZONTAL TAIL DUE TO TRAILING SHOCK WAVES FROM AN AXISYMMETRIC BODY WITH AN EXITING JET

By Reino J. Salmi and John L. Klann

Lewis Flight Propulsion Laboratory
Cleveland, Ohio

NATIONAL ADVISORY COMMITTEE
FOR AERONAUTICS
WASHINGTON

January 25, 1956
Declassified October 31, 1958

NACA RM E55J13a

NATIONAL ADVISORY COMMITTEE FOR AERONAUTICS

RESEARCH MEMORANDUM

# INTERFERENCE EFFECTS AT MACH 1.9 ON A HORIZONTAL TAIL DUE TO TRAILING SHOCK WAVES FROM AN AXISYMMETRIC BODY WITH AN EXITING JET

By Reino J. Salmi and John L. Klann

## SUMMARY

The normal force and pitching moment of a rectangular tail surface at Mach 1.9 were measured to determine the interference effects due to trailing shock waves from an axisymmetric body with a jet exiting from a sonic nozzle in the base. The data were obtained at various jet pressure ratios and locations of the tail with respect to the body. In addition, the effects of the tail shock waves on the body base pressures were obtained.

The results indicated that large variations in the tail normal force resulted from changes in the location at which the shock waves impinged on the tail when the jet pressure ratio was high and the shock waves relatively strong. Equally large changes in the normal force resulted from changes in the shock strength due to increasing the jet pressure ratio when the shock waves intercepted a large percentage of the tail area. Increasing the height of the tail reduced the shock interference effects only for the highest position of the range investigated. The afterbody base pressures were significantly increased when the oblique shock waves from the tail leading edge were in the vicinity of the base.

## INTRODUCTION

In locating a horizontal tail surface on a supersonic airplane, it is necessary to consider the interference effects of trailing shock waves from other parts of the airplane. Undesirable changes in the airplane stability and excessive control loads can result from shock-induced forces on the horizontal tail. In reference 1, large jet-induced effects on the longitudinal trim of a free-flight model at Mach numbers between 1.2 and 1.8 are reported. In a study of the actual pressure field on a flat plate due to a trailing shock wave from a circular body (ref. 2), it was

shown that large variations in the surface pressures with severe gradients occurred even for relatively large distances between the origin of the shock wave and the flat plate.

In most cases, the shock waves most likely to interfere with the tail are those trailing behind a fuselage or nacelle. The relative location of the trailing shock waves with respect to the body can vary considerably with the flight Mach number, the airplane attitude, and the jet pressure ratio (if there is a jet exiting from the base of the body).

In order to determine the magnitude and the nature of the shock-wave interference problem for the case of a horizontal tail and an axisymmetric body, an experimental investigation was conducted at the NACA Lewis laboratory in the 18- by 18-inch Mach 1.9 tunnel to measure the normal force and the moment of a rectangular horizontal tail located at various positions behind a body with a jet exiting from a sonic nozzle in the base.

## SYMBOLS

The following symbols are used in this report:

$C_m$ pitching-moment coefficient, $m/qSc$

$C_N$ normal-force coefficient, $N/qS$

$C_p$ pressure coefficient, $(p - p_0)/q$

c tail chord

$M_0$ free-stream Mach number

m pitching moment

N normal force

P total pressure

p static pressure

q dynamic pressure, $\gamma p_0 M_0^2/2$

S tail area

s distance from tail trailing edge to any point along tail chord, in.

x distance from fuselage base, positive in downstream direction, in.

y distance from fuselage centerline, in.

$\gamma$ ratio of specific heats of air

Subscripts:

b base

j jet

s shock vertex intercept point

t tail leading edge

0 free-stream conditions

## APPARATUS AND TESTS

The geometric characteristics of the tail and the fuselage are shown in figure 1. The tail was made from mild steel and soldered to the strain-gage sting support. The fuselage was supported in the tunnel by a vertical strut which also formed the passage for the air to a convergent nozzle in the base. An internal rake in the fuselage was used to measure the total pressure of the jet. A photograph of the fuselage and tail in the tunnel is shown in figure 2.

The tests were made in the 18- by 18-inch Mach 1.9 wind tunnel, which exhausts heated and dried atmospheric air and has a normal operating Reynolds number of about $3.38\times10^6$ per foot. A dew point of $-5^\circ$ or less and a tunnel total temperature of $150^\circ$ F was maintained to prevent condensation effects. The strain-gage readings for the normal force and the pitching moment were recorded in addition to the fuselage base pressures and the usual tunnel operating conditions. Surveys were made for nominal jet pressure ratios $P_j/p_0$ ranging from jet-off to about 11 at various tail heights and horizontal positions with the tail at zero angle of attack. A few tail positions were investigated with the jet pressure ratio set at 16.

A thermocouple which was mounted to the strain-gage body indicated an effect of temperature on the strain-gage readings. The temperature effects were minimized, however, by allowing the gages to reach an equilibrium temperature before the data were recorded. The no-load strain-gage readings were also obtained at the operating temperature by rapidly closing the tunnel upstream valve and recording the wind-off readings before an appreciable amount of cooling had occurred. The overall accuracy of the normal-force coefficient varied with the tail load and was estimated to be of the order of 0.01 at the largest values of

$C_N$. This included the effects of temperature, the sensitivity of the strain-gage system used, and the tail bending due to load. The corresponding accuracy in the pitching-moment coefficient, which also decreased with increasing $C_N$, was of the order of 0.02 at the maximum value of $C_N$ measured.

The loads resulting from interference effects on the tail due to the support shroud and from pressures on the support sting were not measured. From numerous schlieren photographs and observations of the schlieren during the tests, it was concluded that the interference effects of the shroud on the loading of the tail were very small relative to the test accuracy and were probably nonexistent. For all cases, the normal shock due to the support shroud was at the shroud inlet. The shroud probably acted as a normal-shock inlet because of leakage of air from the sides of the shroud. The boundary layer on the sting ahead of the shroud did not appear to be separated or adversely affected by the shock at the shroud. Pressure differences above and below the sting within the shroud should be negligibly small because of the low air velocities within the shroud.

## RESULTS AND DISCUSSION

Trailing shock waves from a fuselage can produce variations in the tail normal-force coefficient either by a change in the position of impingement on the tail or by a change in the shock strength. For a fixed fuselage and tail arrangement, the relative location of the trailing shock wave from the fuselage varies with the free-stream Mach number, the airplane angle-of-attack, and the jet pressure ratio (if there is a jet exiting from the base of the fuselage). The strength of the shock wave is mainly a function of the free-stream Mach number and the jet pressure ratio. Of these parameters, only the jet pressure ratio was varied in the present investigation.

The effect of the jet pressure ratio on the position of the trailing shock waves relative to the fuselage afterbody is shown in figure 3. These shock positions were measured from schlieren photographs. The fuselage afterbody had a blunt base with a ratio of jet to base diameter of 0.714. With the jet off and at low jet pressure ratios, the sudden turning of the stream flow around the corner of the base resulted in an expansion region just ahead of the first trailing shock wave. When the jet pressure ratio was increased, the increased expansion of the jet from the sonic nozzle moved the first shock wave forward and reduced free-stream expansion around the corner. The second trailing shock wave, which originated from the normal shock in the jet stream, moved further downstream with increasing jet pressure. The schlieren photographs indicate that the flow area between the first and second shock waves was fairly uniform.

In the present case a convergent exit nozzle was used. For other nozzle types, such as convergent-divergent nozzles, and a similar afterbody, the position of the first shock wave would correlate more closely to the positions for the sonic nozzle at equal jet-exit static-pressure ratios. The ratio of nozzle diameter to base diameter would also influence the manner in which the jet pressure ratio affects the strength and position of the trailing shock wave. The schlieren photographs indicate that the interaction of the oblique-shock wave from the tail leading edge did not cause a measurable change in the position of the fuselage trailing shock wave.

The measured interference effects resulting from the intersection of the trailing shock waves with the tail surface also include the effects of the flow field behind the shock wave. The flow field between the first and second shock waves is dependent on the jet shape and varies, therefore, with jet pressure ratio. In general, the flow field reduces the pressures downstream of the shock wave. As the shock strength (pressure rise across the shock wave) increases with jet pressure ratio, the expansion effect of the flow field behind the shock wave also increases. The net result, however, is an over-all increase in the pressures on the tail surface affected by the shock wave. In this sense, the jet pressure ratio can be used as an indication of the shock strength.

The variation of the tail normal-force coefficient $C_N$ with the longitudinal position of the tail leading edge relative to the body $x_t$ is presented in figure 4 for various jet pressure ratios and tail heights. The position of the shock intercept as determined from figure 3 is indicated by the line on the x-axes labeled $x_s$. Figure 4 indicates that for a given value of $y$ the variations in the normal-force coefficient for various jet pressure ratios are similar in the region of $-x_t$, which is generally the flow region ahead of the trailing shock waves; whereas in the vicinity of $x_s$ the $C_N$ variations differ considerably through the jet-pressure-ratio range.

A typical example of the variation of the tail normal force with the position of the tail relative to the trailing shock wave is shown in figure 5 for a tail height of 2.86 inches. The letters A and B denote the tail positions where the trailing edge is just ahead of the first shock wave and where the leading edge is just behind the first shock wave, respectively. The second trailing shock wave was at a distance far enough from the first shock wave so that it did not intersect the tail as it was moved from A to B. A large increase in the normal-force coefficient occurred as the tail was moved through the shock wave from A to B. The shock wave probably influenced the pressures on the tail lower surface in a manner similar to that shown in reference 2, which indicates that the pressure rise on the surface of a flat plate due to shock impingement is characterized by a steep high-pressure peak near the point of intersection. The maximum value of $C_N$ occurred before the

tail was completely behind the first shock wave. The decrease in $C_N$ from the maximum value to the value at point B may have resulted from the loss of the high pressure peak from the tail lower surface when the shock wave emerged ahead of the tail leading edge. A slight decrease in $C_N$ also occurred as the tail first entered the trailing shock wave. It is believed that this decline resulted from a decrease in the effective angle of attack at the tail leading edge due to the angularity of the free stream ahead of the shock wave.

The tail normal-force coefficient is shown as a function of the shock-position parameter $s/c$ in figure 6 for various tail heights and at a constant jet pressure ratio of 11.1. Because the shock position was constant, it was necessary to move the tail in order to vary $s/c$. Some variation in the normal force can result, therefore, from the effect of a nonuniform flow field ahead of the shock wave. The magnitude of this effect will be discussed later in this section; and, as will be shown, the effect was small as far as the data in figure 6 are concerned. The increase in $C_N$ with $s/c$ was large for this pressure ratio, being of the order of a $6^\circ$ tail angle-of-attack change. The effect of $s/c$ was somewhat smaller at the highest tail positions tested. For a tail height of 2.86 inches, the effect of $s/c$ was relatively small up to about the midchord point.

As previously pointed out, an expansion region occurred ahead of the first shock wave at low jet pressure ratios. Movement of the tail leading edge through the expansion region can cause variations in the tail normal force which may be greater than those due to shock impingement. At high jet pressure ratios, the expansion region is diminished and the effect on the normal force may be relatively small. In figure 7, the normal-force coefficient is presented as a function of the jet pressure ratio for various values of $s/c$. At $s/c = 0$, the tail is completely ahead of the first shock wave; and as the pressure ratio is increased, it is necessary to move the tail forward as the shock wave moves forward. An increase in $C_N$ of about 0.024 occurred between jet off and a jet pressure ratio of 4.5. Further increase in the jet pressure ratio to a value of 11.1 then resulted in a decrease in the value of $C_N$ of about 0.014.

This variation in the $C_N$ curve can be explained by an examination of the flow angularity at a constant value of $y$. Expansion of the free-stream flow around the initial boattail break results in a region of increasing downwash. Compression along the boattail reduces the downwash to the point where the expansion around the corner of the base at low jet pressure ratios again increases the downwash just ahead of the first trailing shock wave. When the tail position is maintained just ahead of the first shock wave ($s/c = 0$), it must be moved forward when the jet pressure ratio is increased. The sudden expansion around the boattail break induces a download on the tail which is at a maximum with

the jet off. Increasing the jet pressure ratio reduces the expansion around the base, and the normal-force coefficient increases. When the expansion is completely eliminated, the tail is influenced mainly by the flow over the boattail, which tends to increase the download on the tail when it is moved forward.

From figure 7 it can be seen that at low jet pressure ratios the downforce $-C_N$ increases as $s/c$ is increased. This emphasizes the fact that at low jet pressure ratios the effects of shock impingment are small and are overshadowed by the effects of moving the tail so that it is influenced by the expansion ahead of the shock wave. At high jet pressure ratios it is evident that the effects of shock impingment predominate.

The combined effects of increased shock strength and forward movement of the shock wave on the tail lower surface are shown in figure 8 along with the corresponding curve for a constant high jet pressure ratio. Figure 8 also shows that at low values of $s/c$ the shock strength has relatively small effect on the normal force.

The effects of $s/c$ may vary with the tail plan form. In the present case, a rectangular tail was employed. For a sweptback tail, the effects of shock movement may be more severe, because the sweptback plan form conforms more closely to the parabolic line of intersection of the trailing shock wave on a horizontal surface (ref. 2). Conversely, a sweptforward tail may exhibit smaller effects of the shock movement.

## Tail Location

The effects of jet pressure ratio on the normal-force coefficient for various horizontal and vertical positions of the tail are shown in figure 9. For a given vertical position (constant $y$) it can be seen that, as the distance of the tail leading edge downstream of the base $x_t$ is increased beyond a certain point, the variation of $C_N$ with jet pressure ratio becomes large. In most cases, however, the total change of $C_N$ with jet pressure ratio remains small (less than 0.03, which corresponds to an effective tail angle-of-attack change of about $1^\circ$) until a jet pressure ratio of about 4.5 is reached. If an arbitrary limit of 0.03 is placed on the variation of the normal-force coefficient, a region where the incremental change in the normal-force coefficient $C_N$ does not vary more than 0.03 with jet pressure ratio for the range from jet off to 4.5 can be defined. This is shown in figure 10, which also indicates the relative locations of the first and second trailing shock waves at a jet pressure ratio of 4.5. The area in which the variation of the normal-force coefficient would be greater than the specified limit parallels the trailing shock waves as would be expected. It can be seen that the area is greater nearer the jet centerline.

The tests were made for a case where the fuselage was at zero angle of attack. Since there would be some movement of the relative shock position with angle of attack, the actual restricted area for this Mach number would probably be somewhat greater.

## Tail Pitching Moment

Figure 11 shows the variation of the tail pitching moment with $x_t$ for various values of $y$ and the jet pressure ratio. In general, the variations in the pitching moment were less severe than those of the corresponding normal-force values. These data are presented mainly to indicate the order of magnitude of the possible variations in the pitching moment.

Since the accuracy of the $C_m$ data is of the order of 0.02 at the highest values of $C_N$ measured, the detailed variation of the $C_m$ curves may not be of practical importance, but the trends should be applicable.

## Tail-Shock-Wave Effects on Base Pressure

The effect of the trailing shock wave from the lower surface of the tail on the base pressure of the fuselage is shown in figure 12. Most of the data were obtained from an orifice located at the bottom of the base. Additional base taps added later in the tests indicated that the circumferential base pressure distribution was fairly uniform.

Significant increases in the base pressure coefficient were evident, especially for the higher tail positions. With the jet on, the maximum increase in the base pressure generally occurred when the shock intercepted the body at a point just ahead of the base; whereas for jet off, it occurred when the shock was slightly downstream of the base. The tail position at which the shock wave intercepts the top edge of the base is also indicated in figure 12. The larger effect for the higher tail positions is attributed to a stronger shock wave from the lower surface of the tail due to a decrease in the downwash angle as $y$ is increased.

## SUMMARY OF RESULTS

Tests at Mach 1.9 of a rectangular tail surface behind a circular body with a jet exiting from the base indicated that

1. When the trailing shock wave from the fuselage intersected the tail surface, large variations in the tail normal force resulted from movement of the shock wave relative to the tail for high jet pressure ratios and from changes in shock strength due to increasing the jet

pressure ratio when a large area of the tail was intercepted by the shock waves.

2. The effects of the shock-wave interference diminished only at the highest tail position in the range tested.

3. The trailing shock waves from the tail leading edge induced significant increases in the base pressures on the body when the shock wave was near the base.

Lewis Flight Propulsion Laboratory
National Advisory Committee for Aeronautics
Cleveland, Ohio, October 19, 1955

## REFERENCES

1. Peck, Robert F.: Jet Effects on Longitudinal Trim of an Airplane Configuration Measured at Mach Numbers Between 1.2 and 1.8. NACA RM L54J29a, 1955.

2. Bressette, Walter E.: Investigation of the Jet Effects on a Flat Surface Downstream of the Exit of a Simulated Turbojet Nacelle at a Free-Stream Mach Number of 2.02. NACA RM L54E05a, 1954.

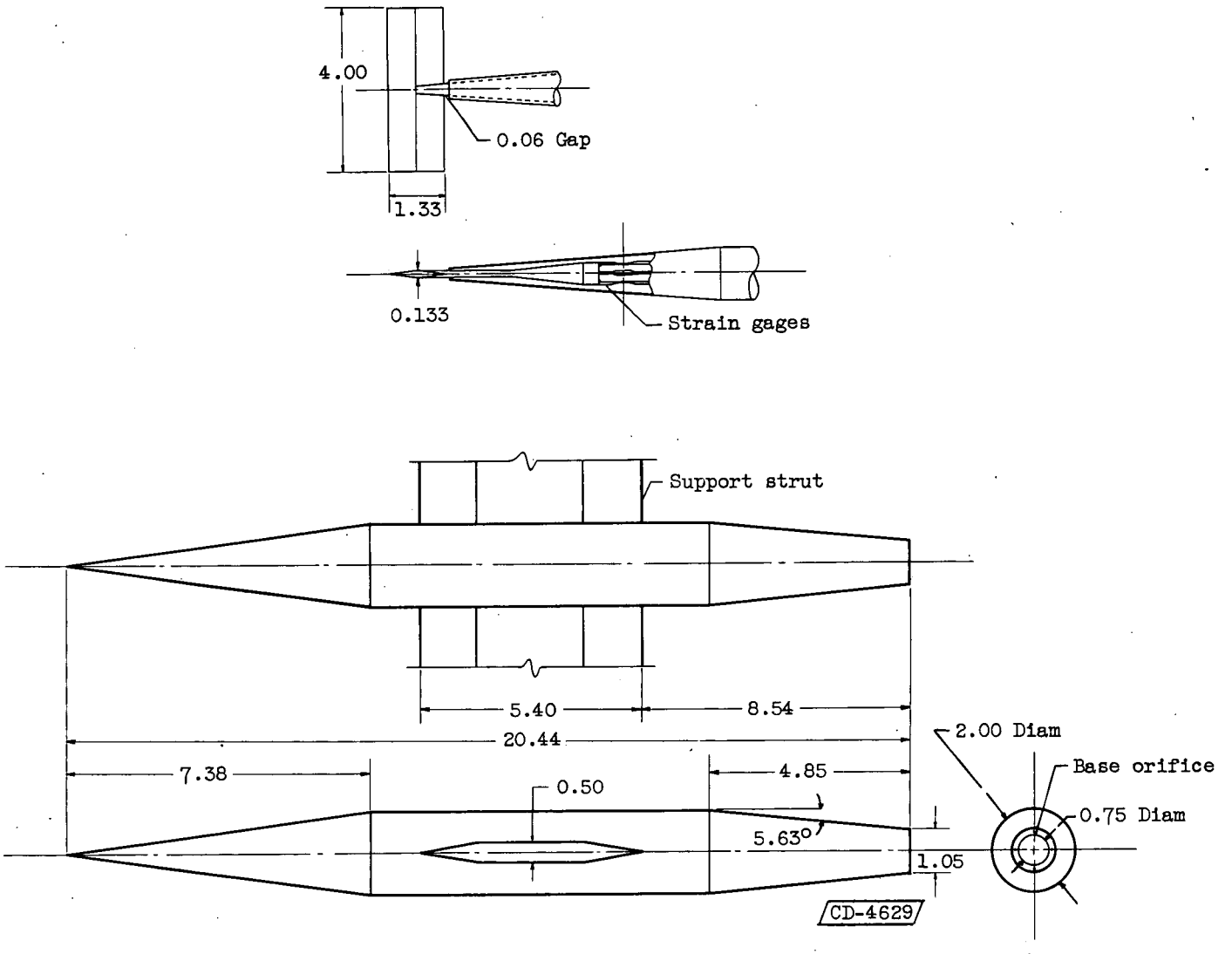


Figure 1. - Model geometry. (All dimensions in inches except as noted.)

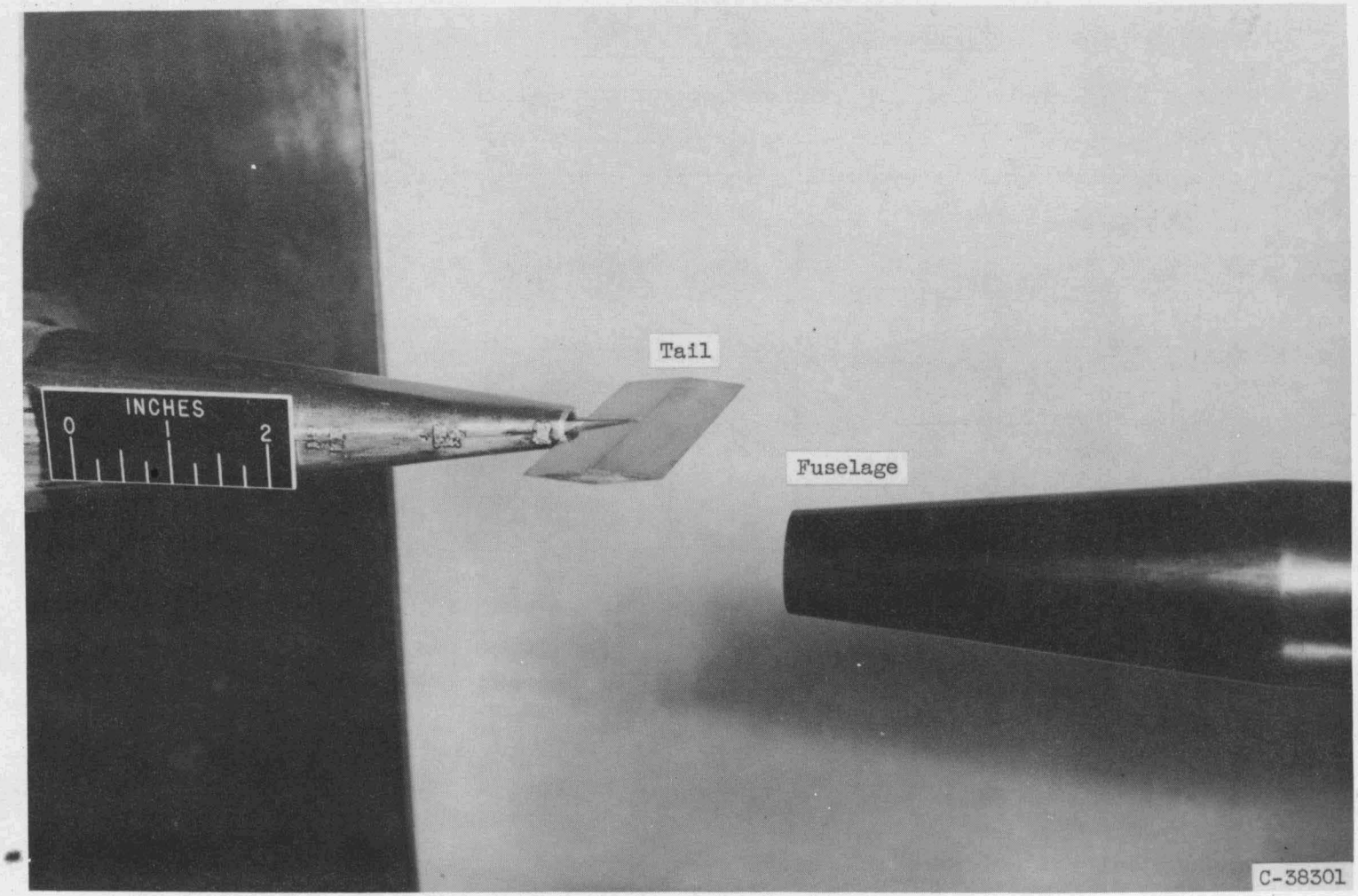


Figure 2. - Model in the 18- by 18-inch Mach 1.9 wind tunnel.

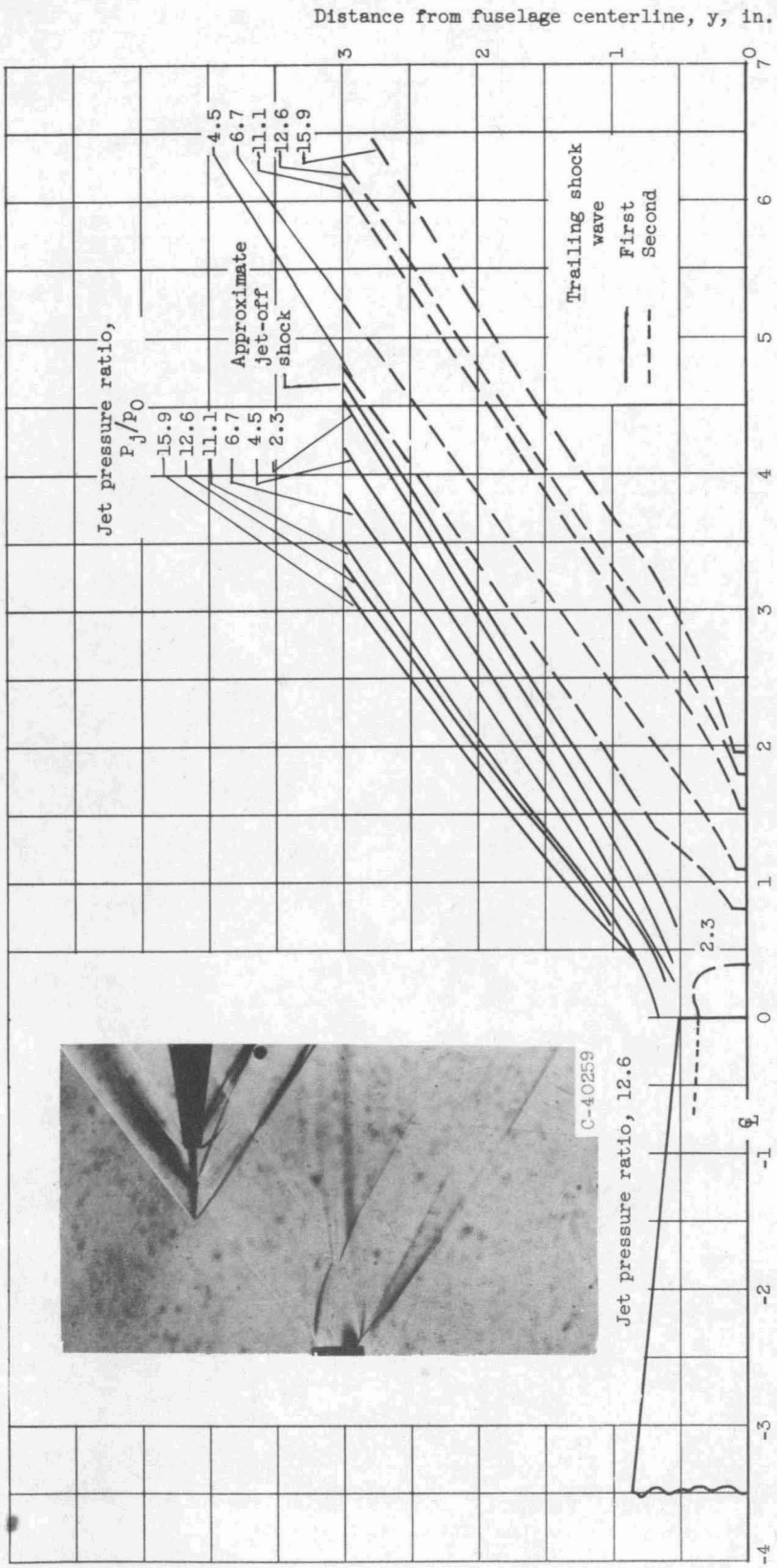


Figure 3. - Effect of jet pressure ratio on trailing-shock-wave location. Free-stream Mach number, 1.9.

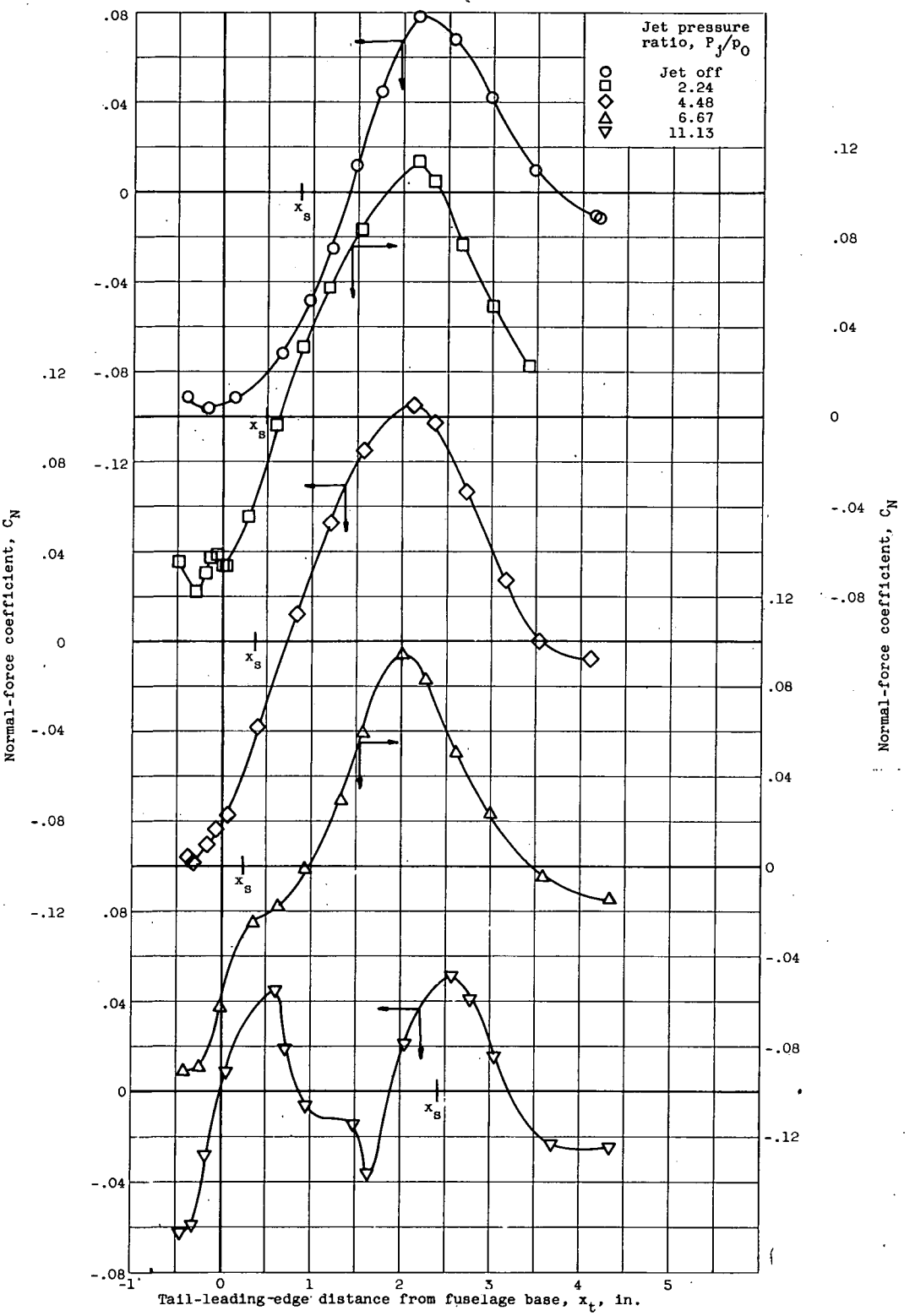


(a) Distance from fuselage centerline, 0.59 inch.

Figure 4. - Effect of tail position on normal-force coefficient.

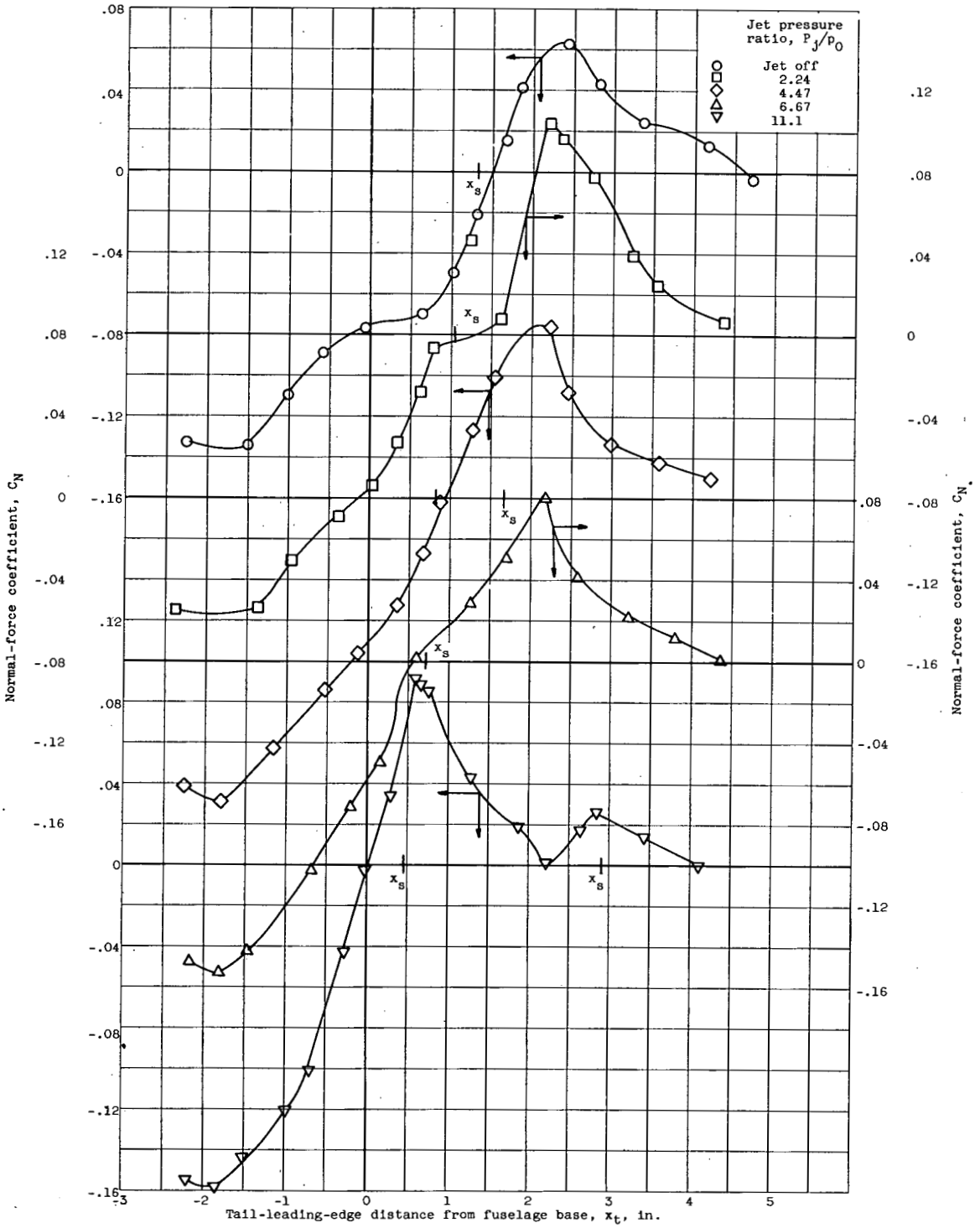


(b) Distance from fuselage centerline, 0.86 inch.

Figure 4. - Continued. Effect of tail position on normal-force coefficient.

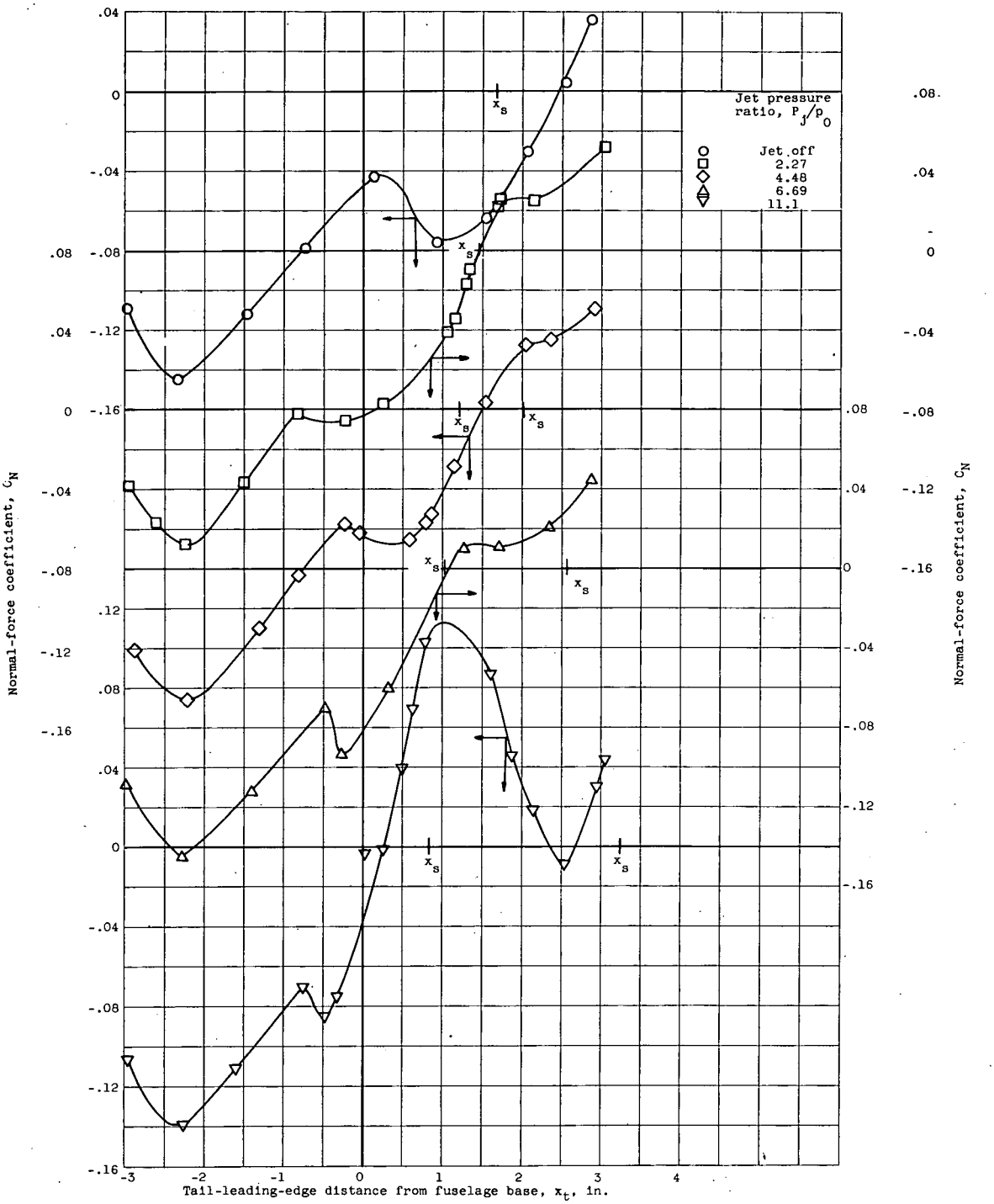


(c) Distance from fuselage centerline, 1.08 inches.

Figure 4. - Continued. Effect of tail position on normal-force coefficient.

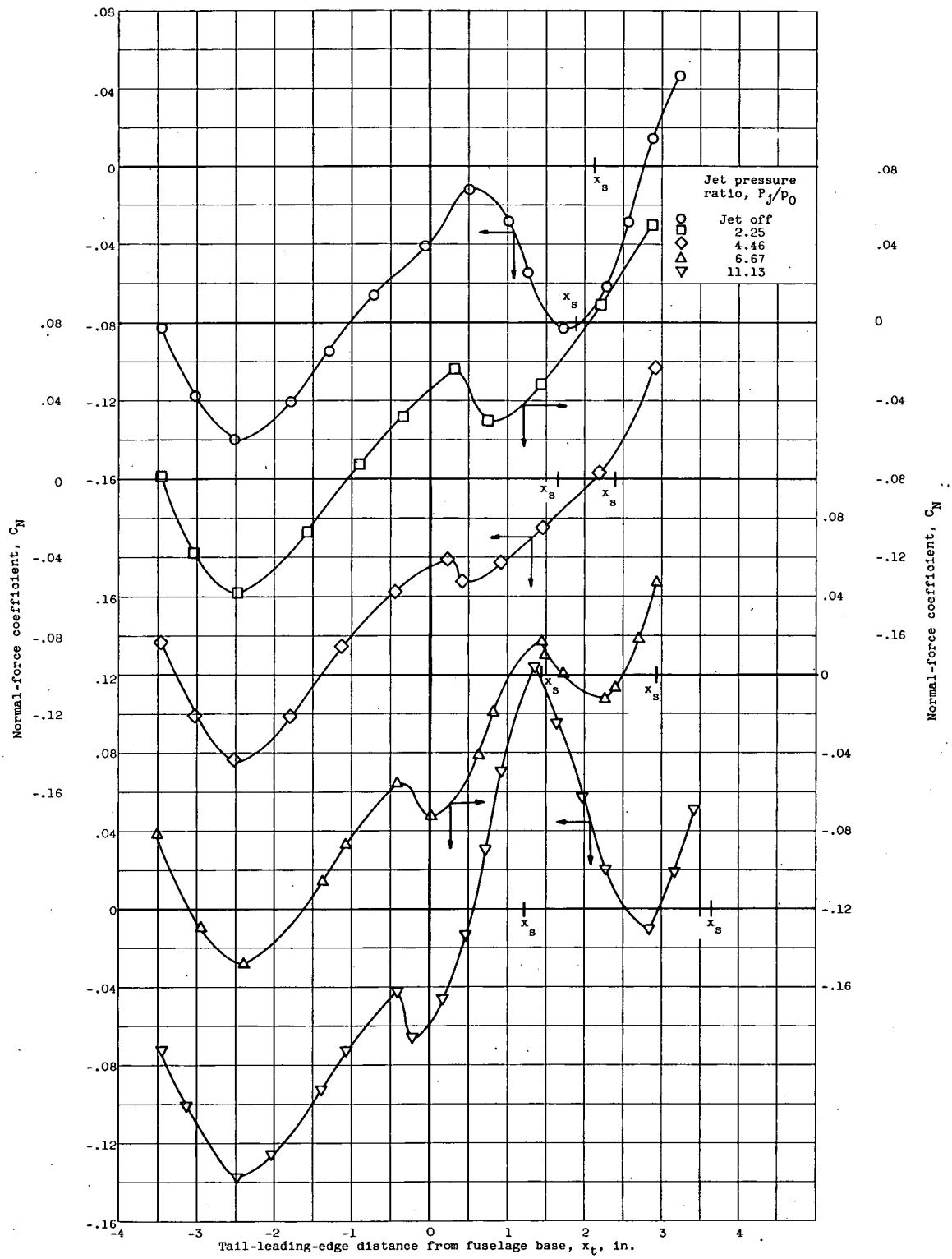


(d) Distance from fuselage centerline, 1.35 inches.

Figure 4. - Continued. Effect of tail position on normal-force coefficient.

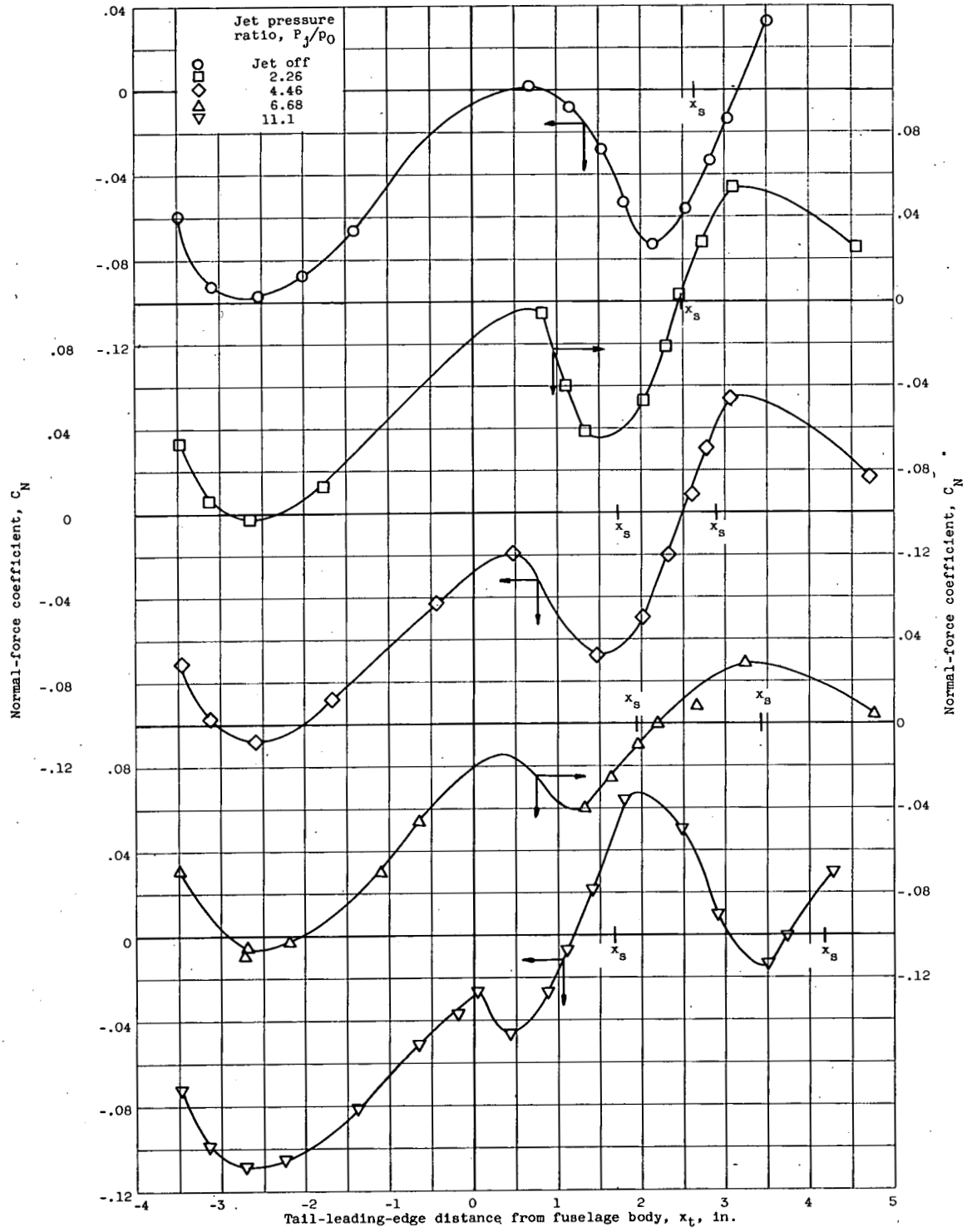


(e) Distance from fuselage centerline, 1.69 inches.

Figure 4. - Continued. Effect of tail position on normal-force coefficient.

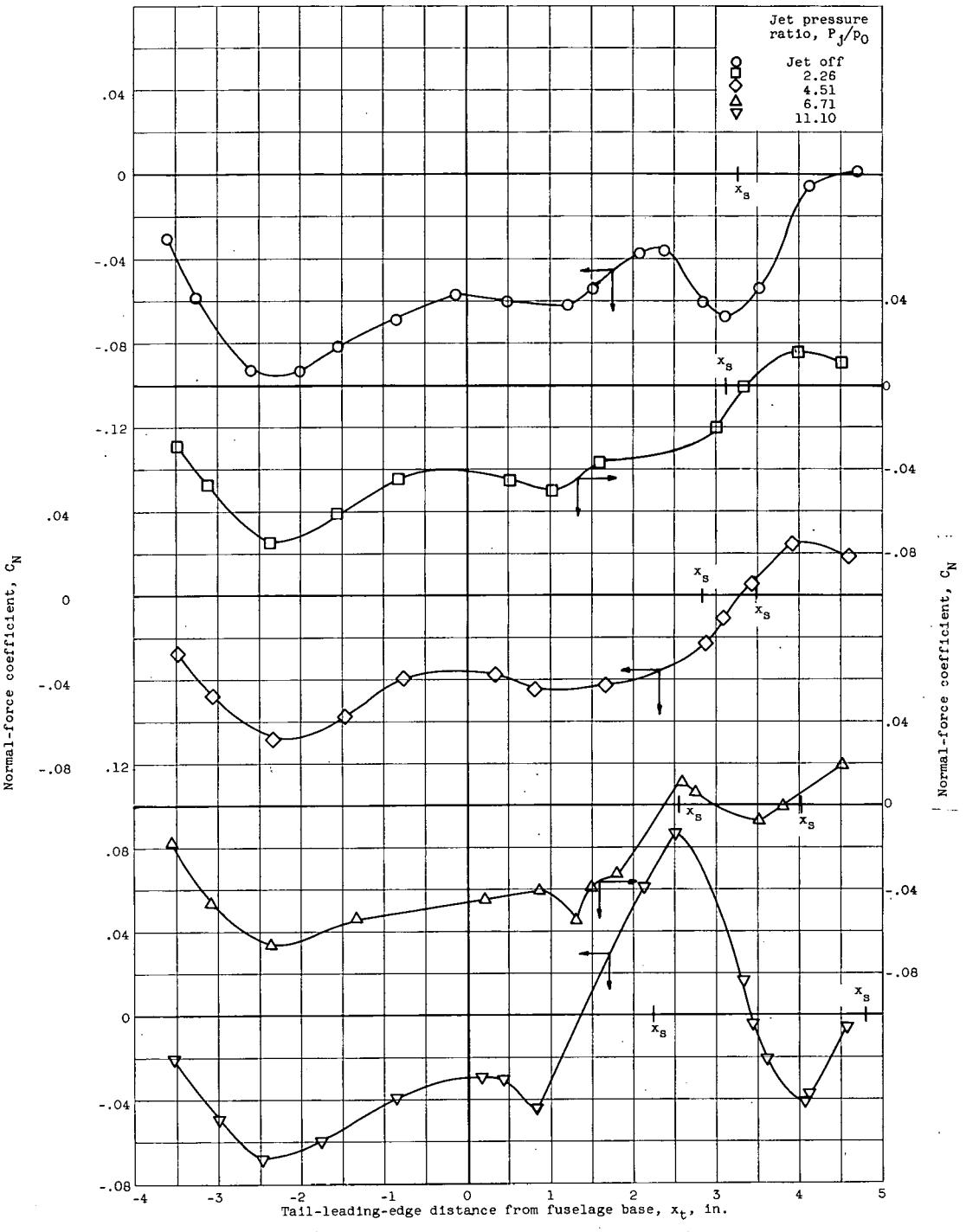


(f) Distance from fuselage centerline, 2.11 inches.

Figure 4. - Continued. Effect of tail position on normal-force coefficient.

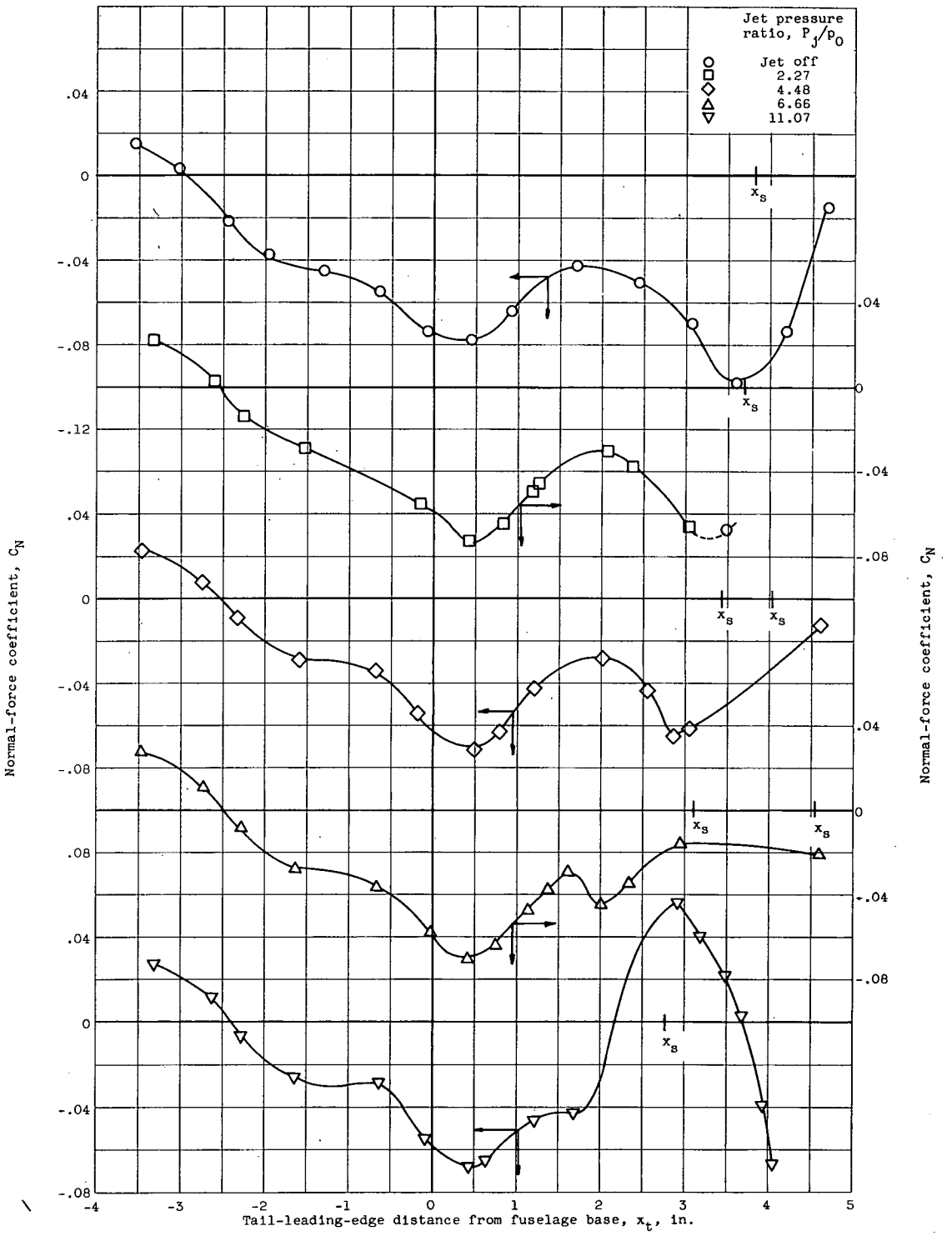


(g) Distance from fuselage centerline, 2.49 inches.

Figure 4. - Continued. Effect of tail position on normal-force coefficient.

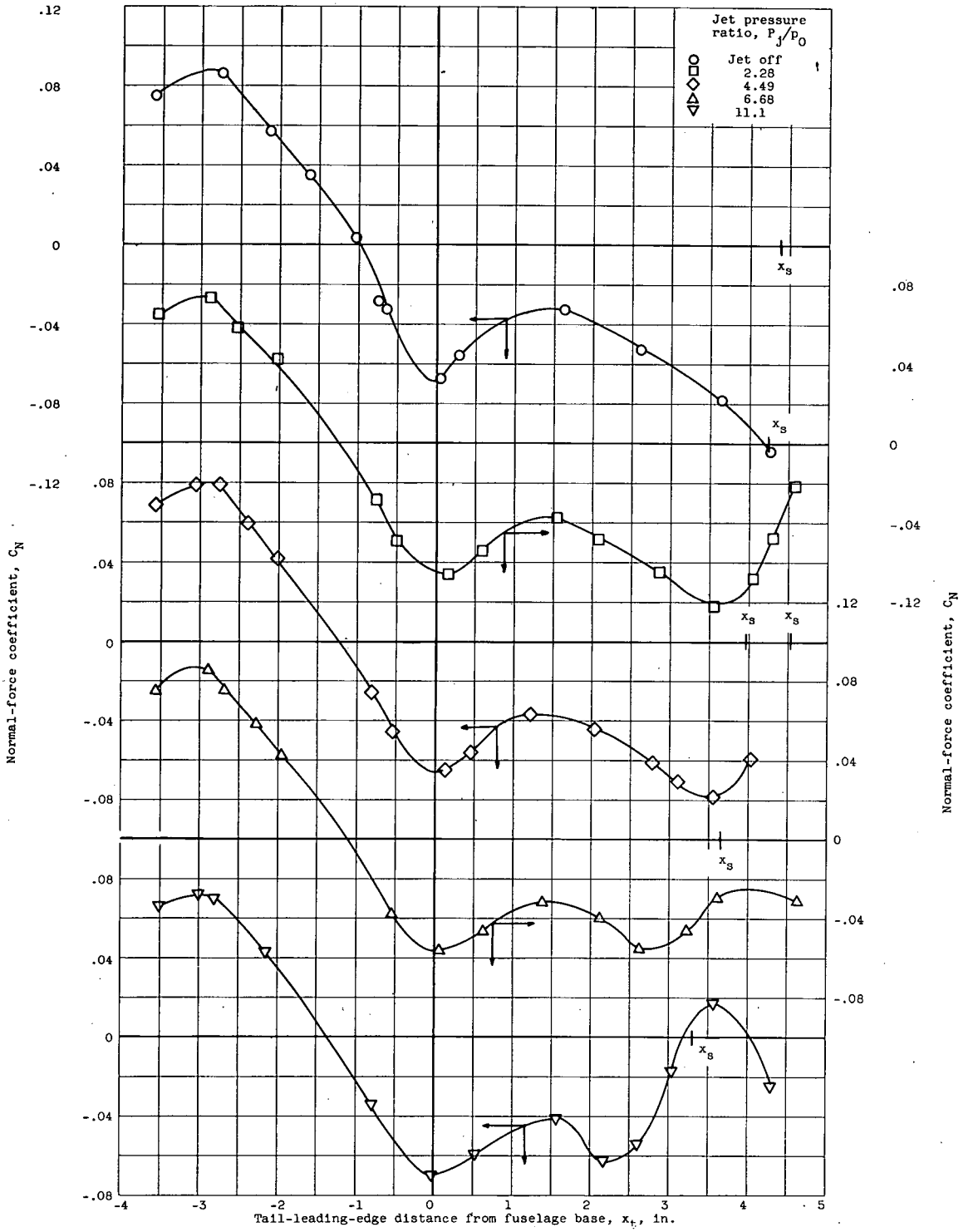


(h) Distance from fuselage centerline, 2.86 inches.

Figure 4. - Concluded. Effect of tail position on normal-force coefficient.

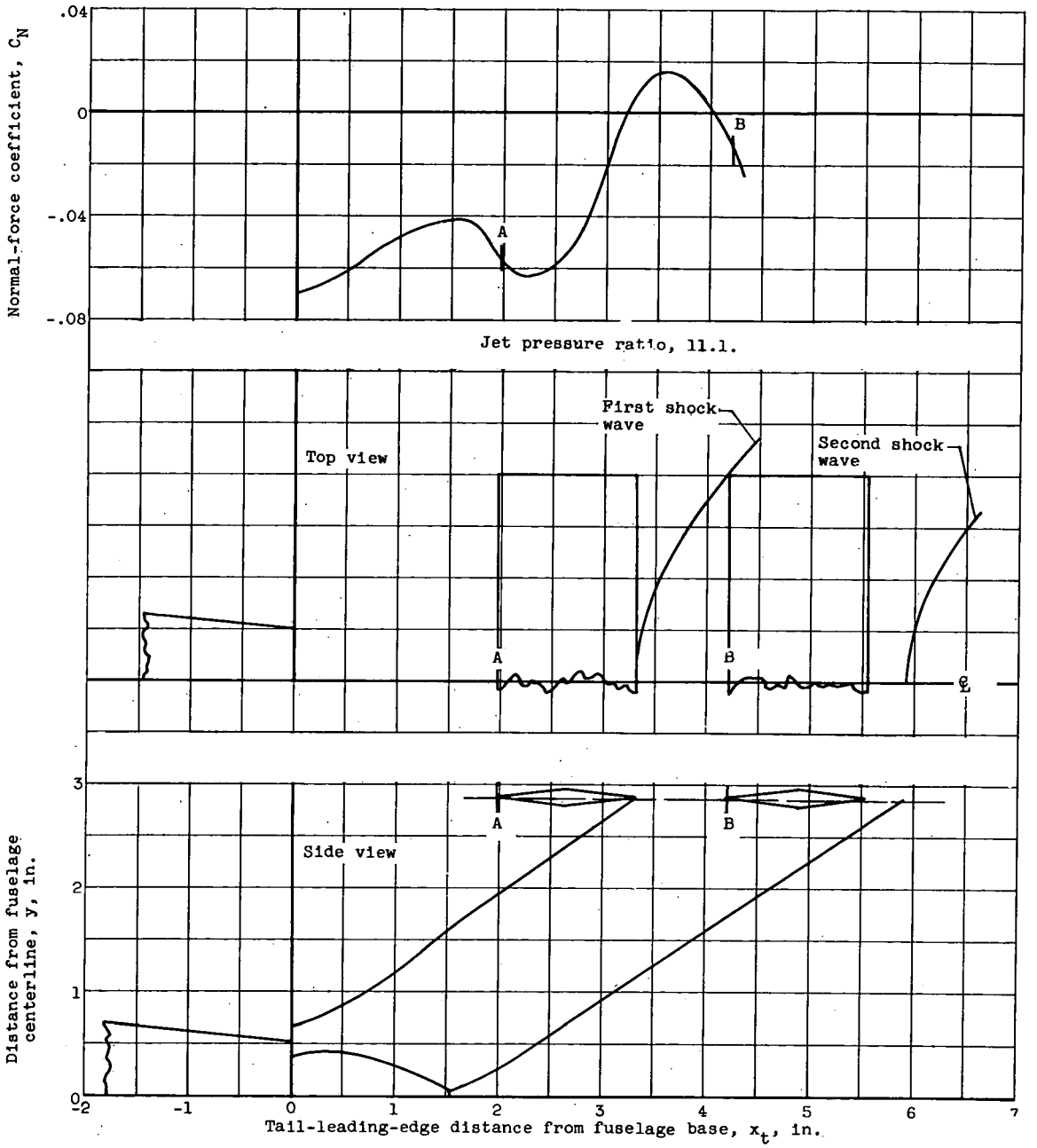


Figure 5. - Relation between normal-force coefficient and shock-wave position. Distance from fuselage centerline, 2.86 inches.

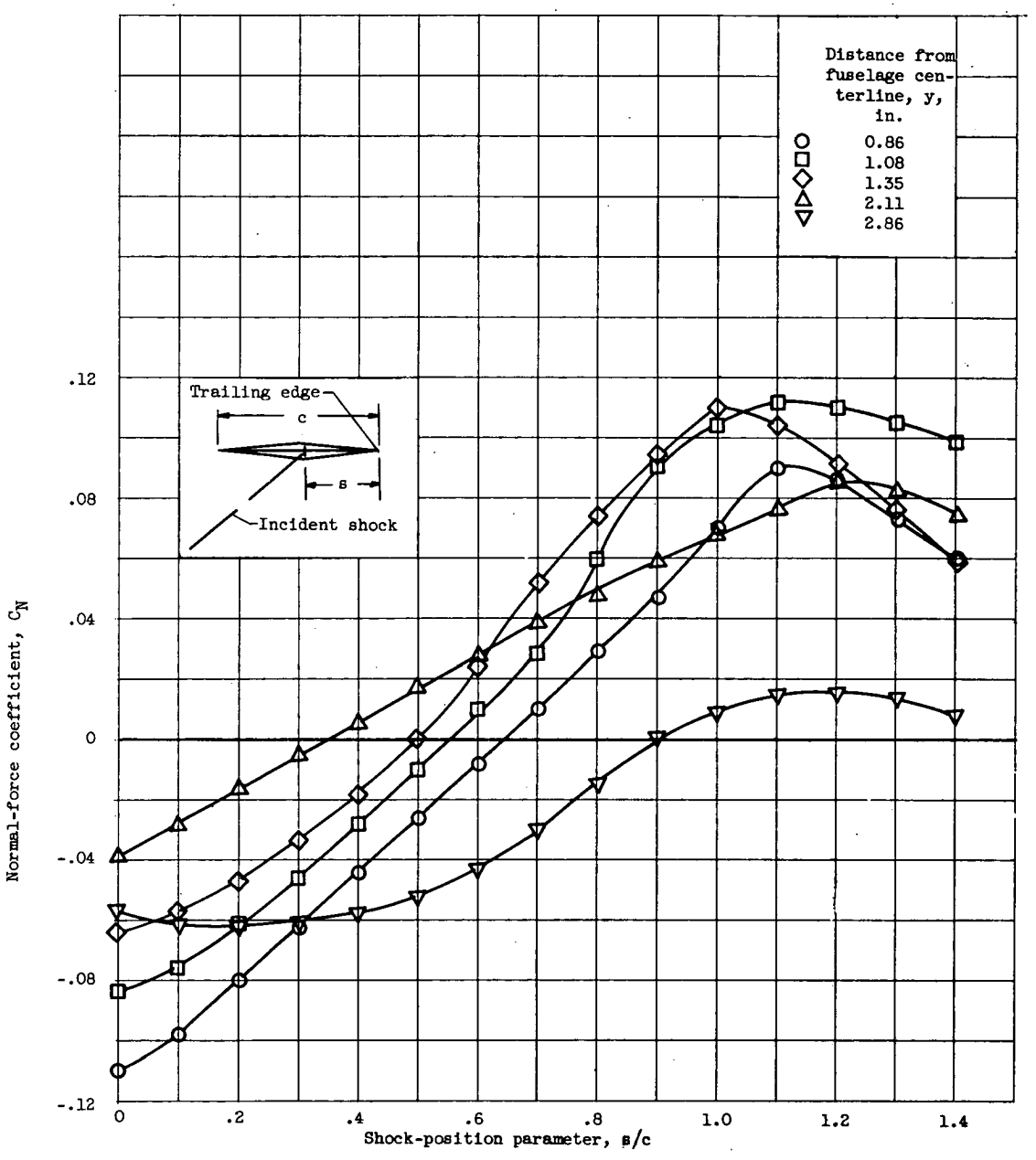


Figure 6. - Effect of shock position on tail normal-force coefficient. Jet pressure ratio, 11.1.

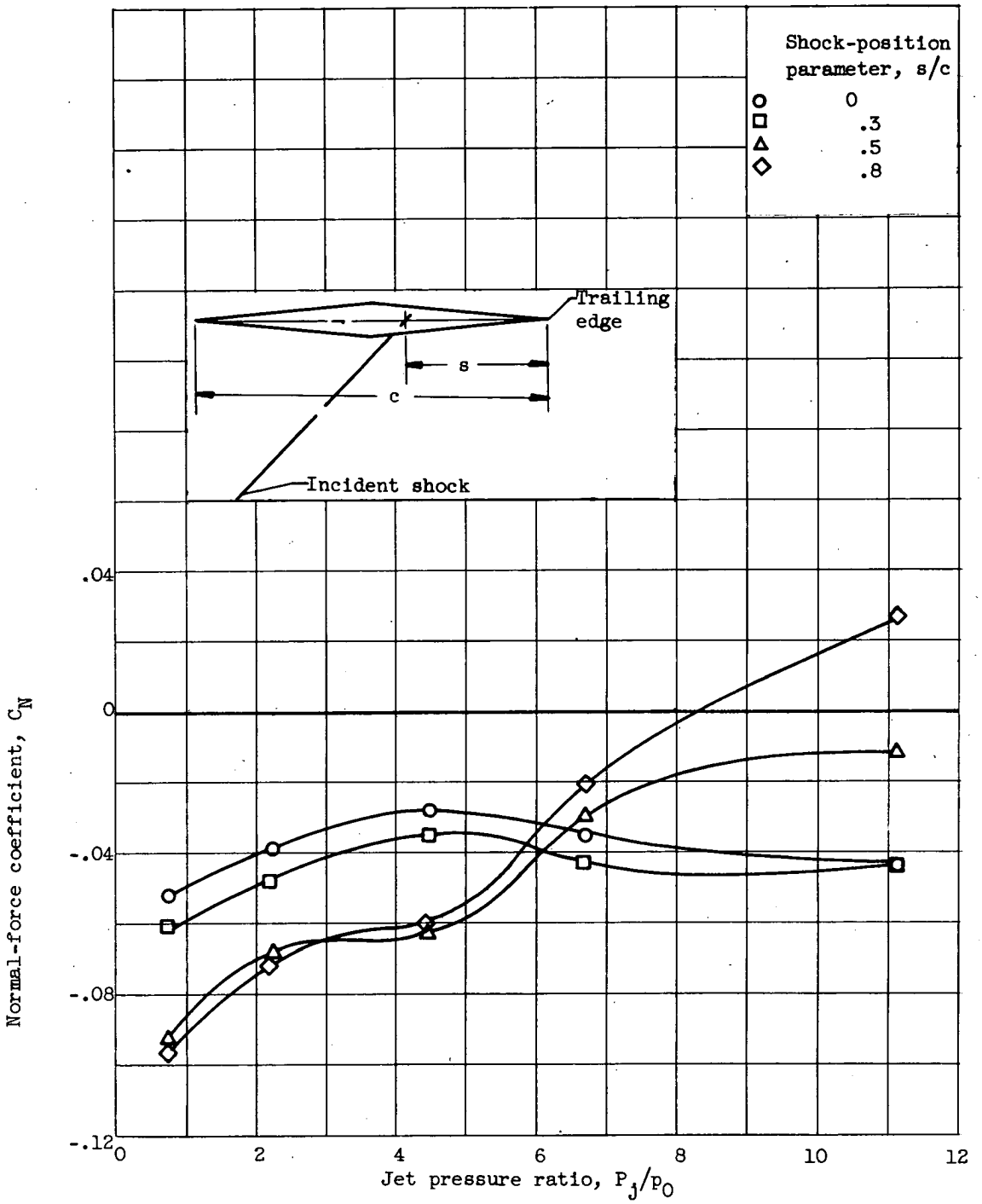


Figure 7. - Effect of shock strength on normal-force coefficient. Distance from fuselage centerline, 2.49 inches.

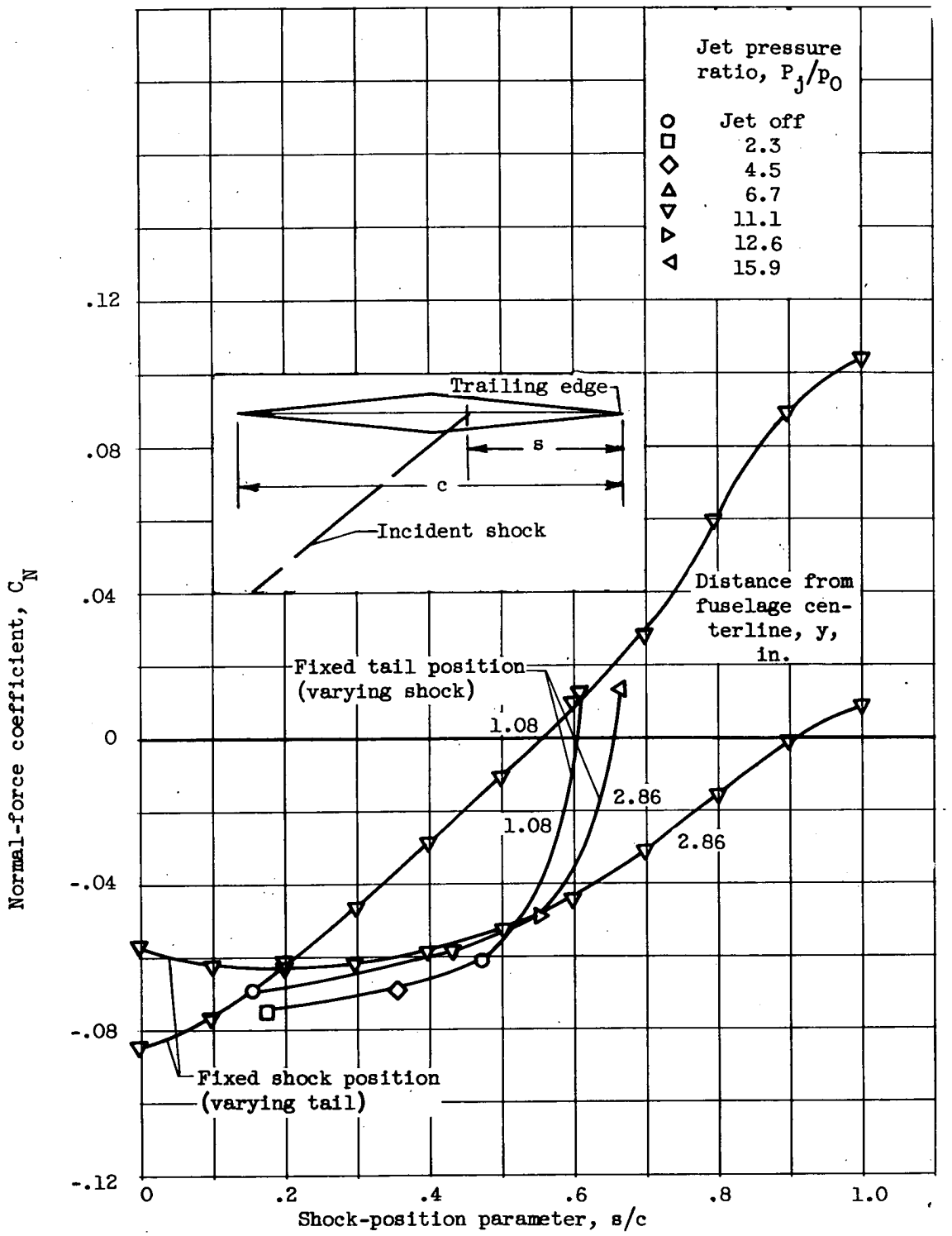


Figure 8. - Effect of shock position on normal-force coefficient for both varying and constant shock positions.

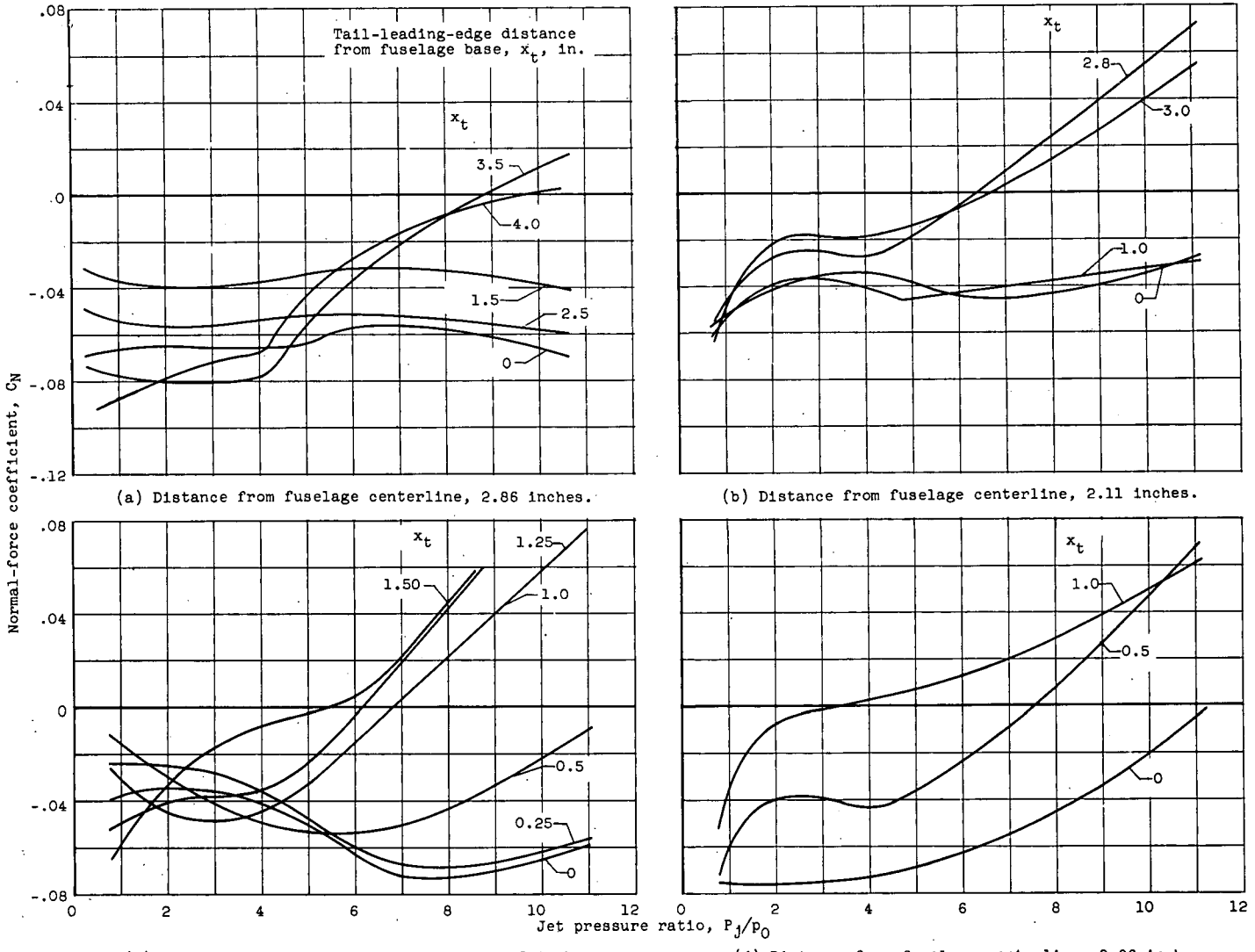


(a) Distance from fuselage centerline, 2.86 inches.

(b) Distance from fuselage centerline, 2.11 inches.

(c) Distance from fuselage centerline, 1.35 inches.

(d) Distance from fuselage centerline, 0.86 inch.

Figure 9. - Variation of tail normal-force coefficient with jet pressure ratio

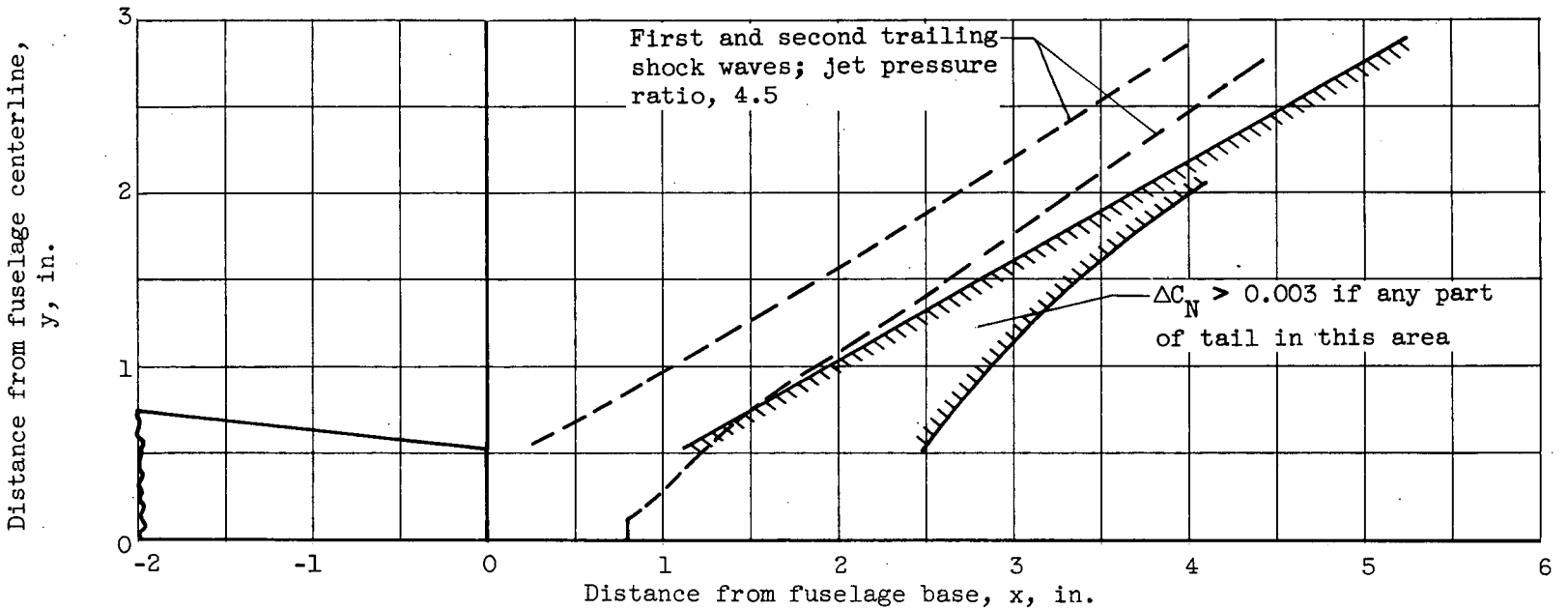


Figure 10. - Limits of tail position for $\Delta C_N \leq 0.03$ for jet pressure ratios varying from jet off to 4.5. $C_N$, normal-force coefficient.

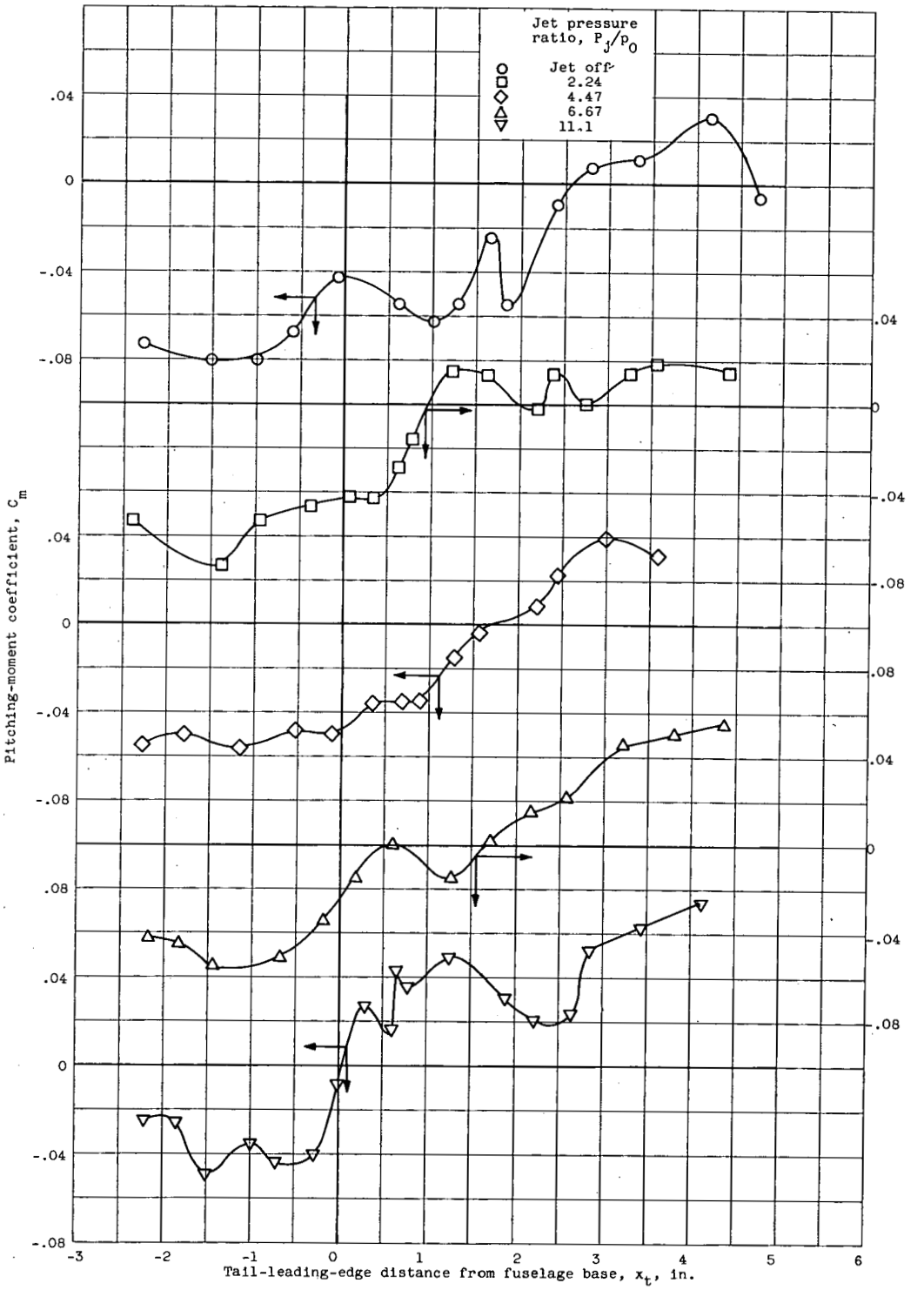


(a) Distance from fuselage centerline, 0.86 inch.

Figure 11. - Variation of pitching-moment coefficient with tail-leading-edge distance from fuselage base.

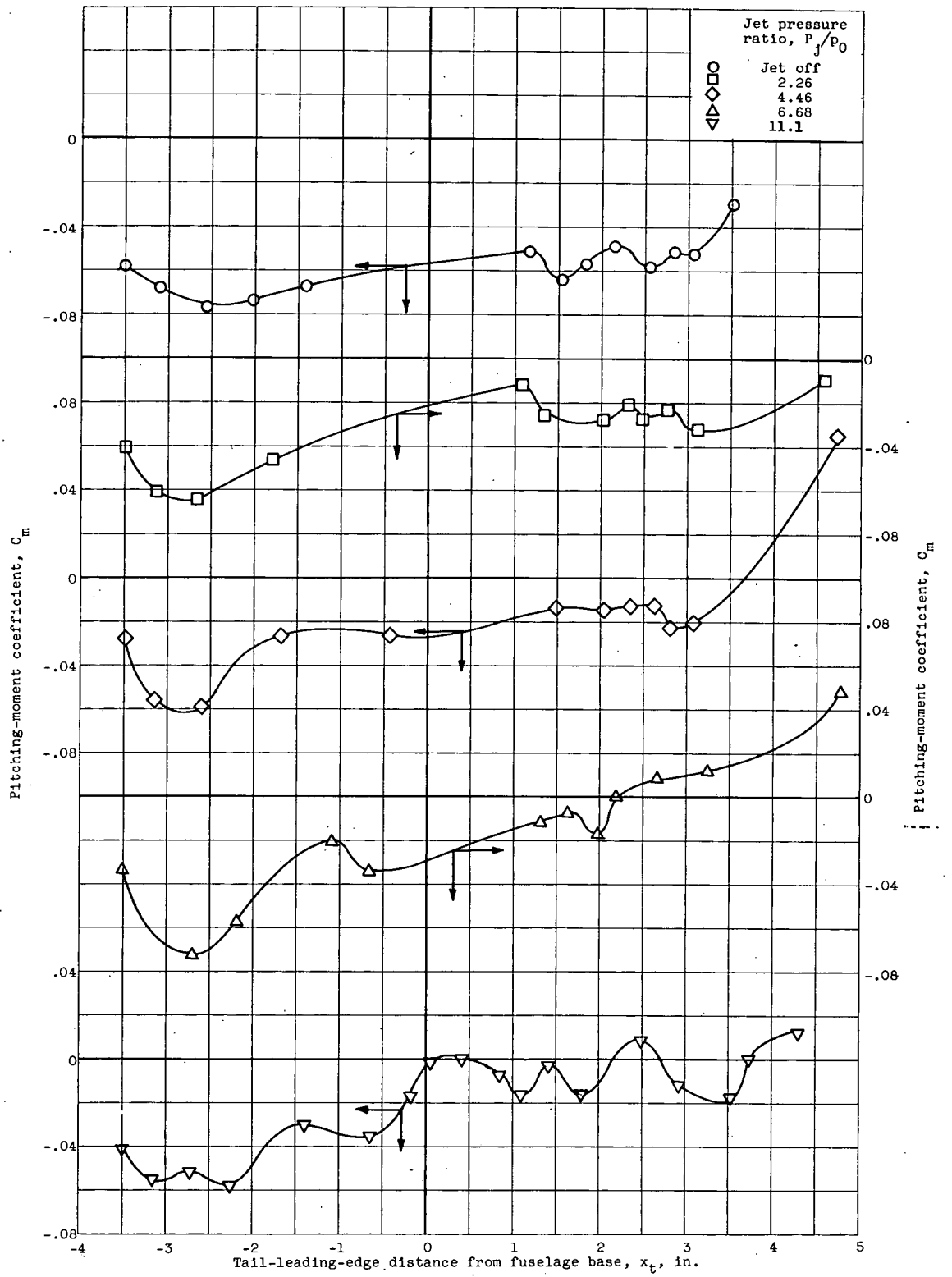


(b) Distance from fuselage centerline, 1.69 inches.

Figure 11. - Continued. Variation of pitching-moment coefficient with tail-leading-edge distance from fuselage base.

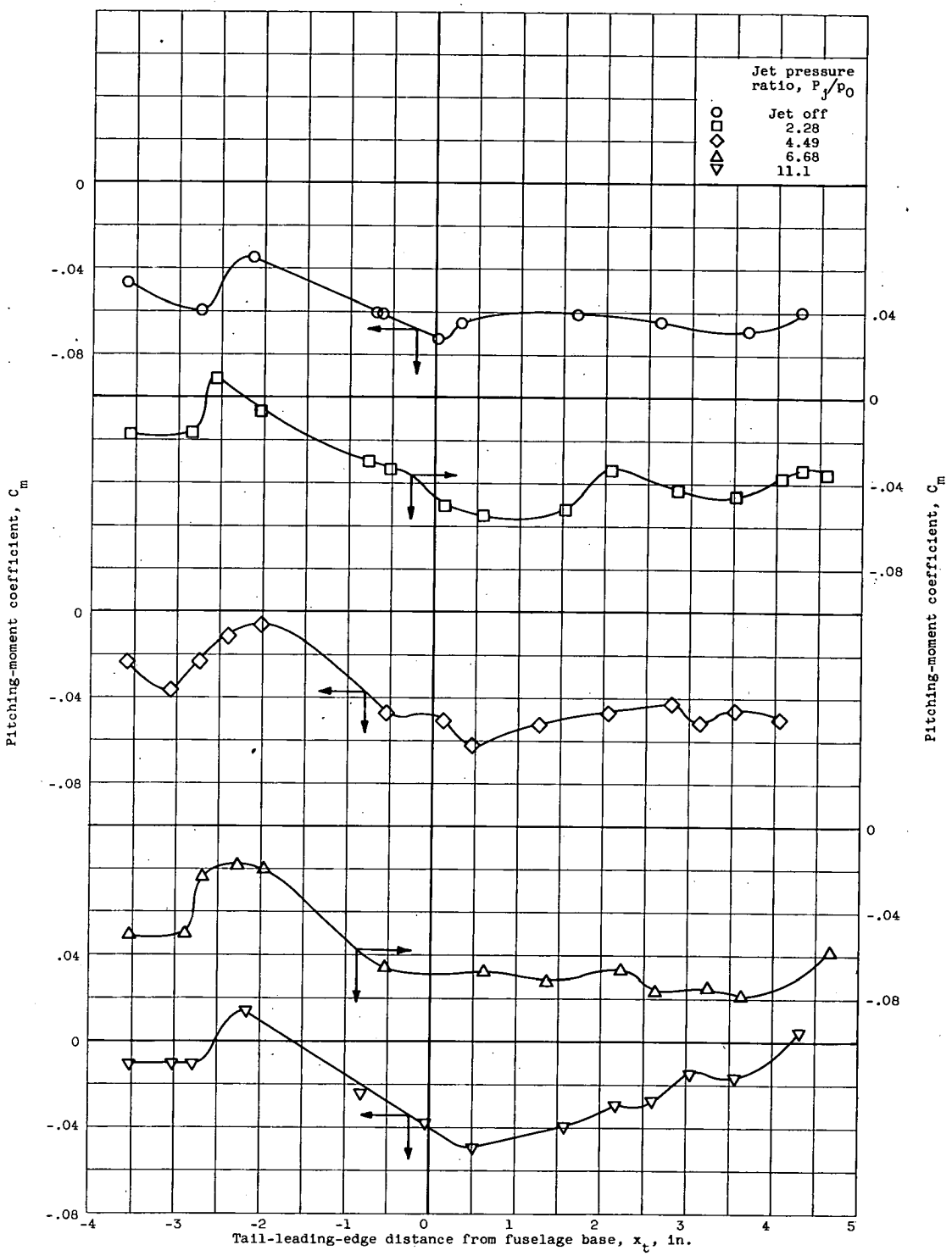


(c) Distance from fuselage centerline, 2.86 inches.

Figure 11. - Concluded. Variation of pitching-moment coefficient with tail-leading-edge distance from fuselage base.

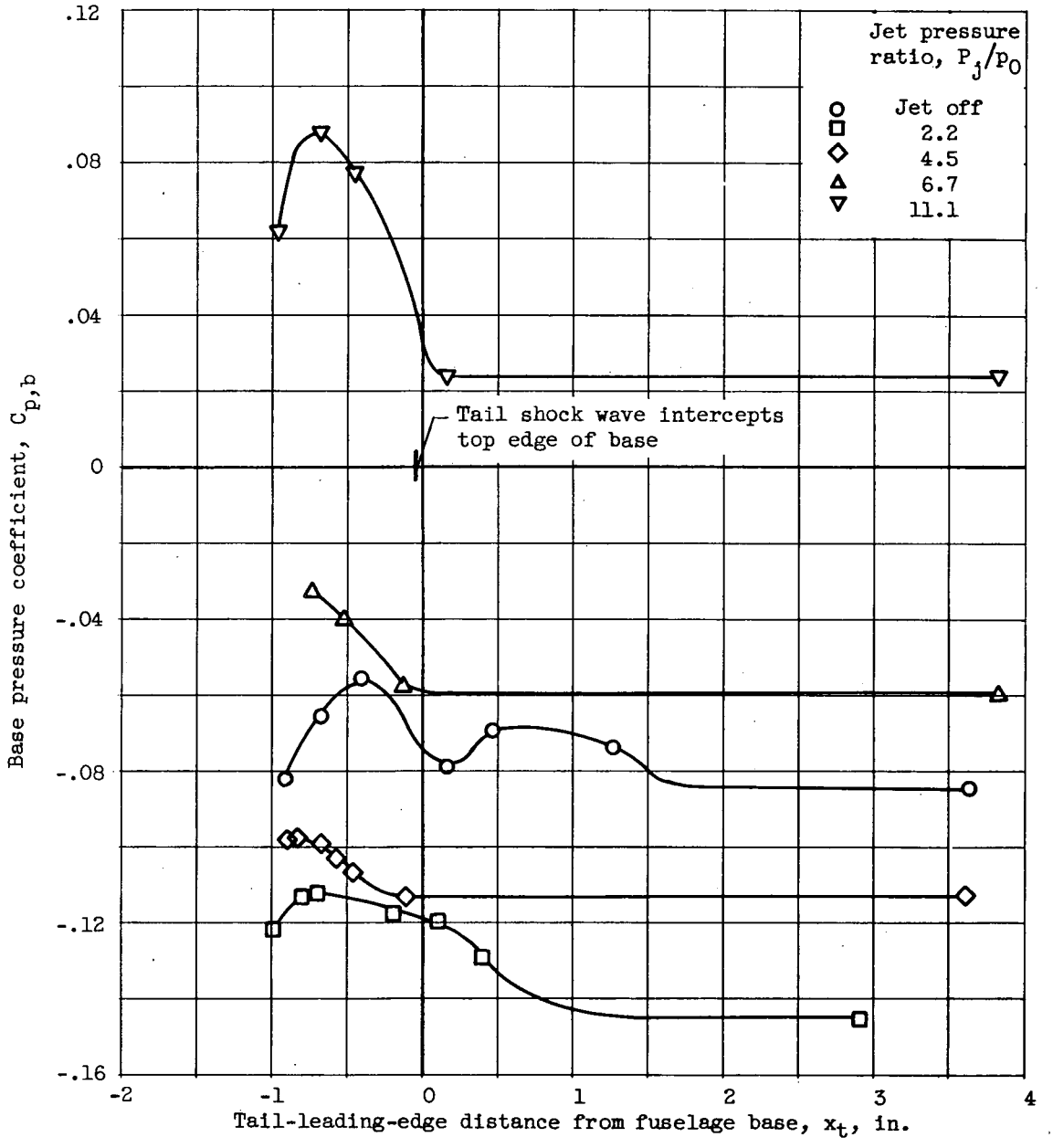


(a) Distance from fuselage centerline, 0.59 inch.

Figure 12. - Effect of tail shock wave on base pressure coefficient.

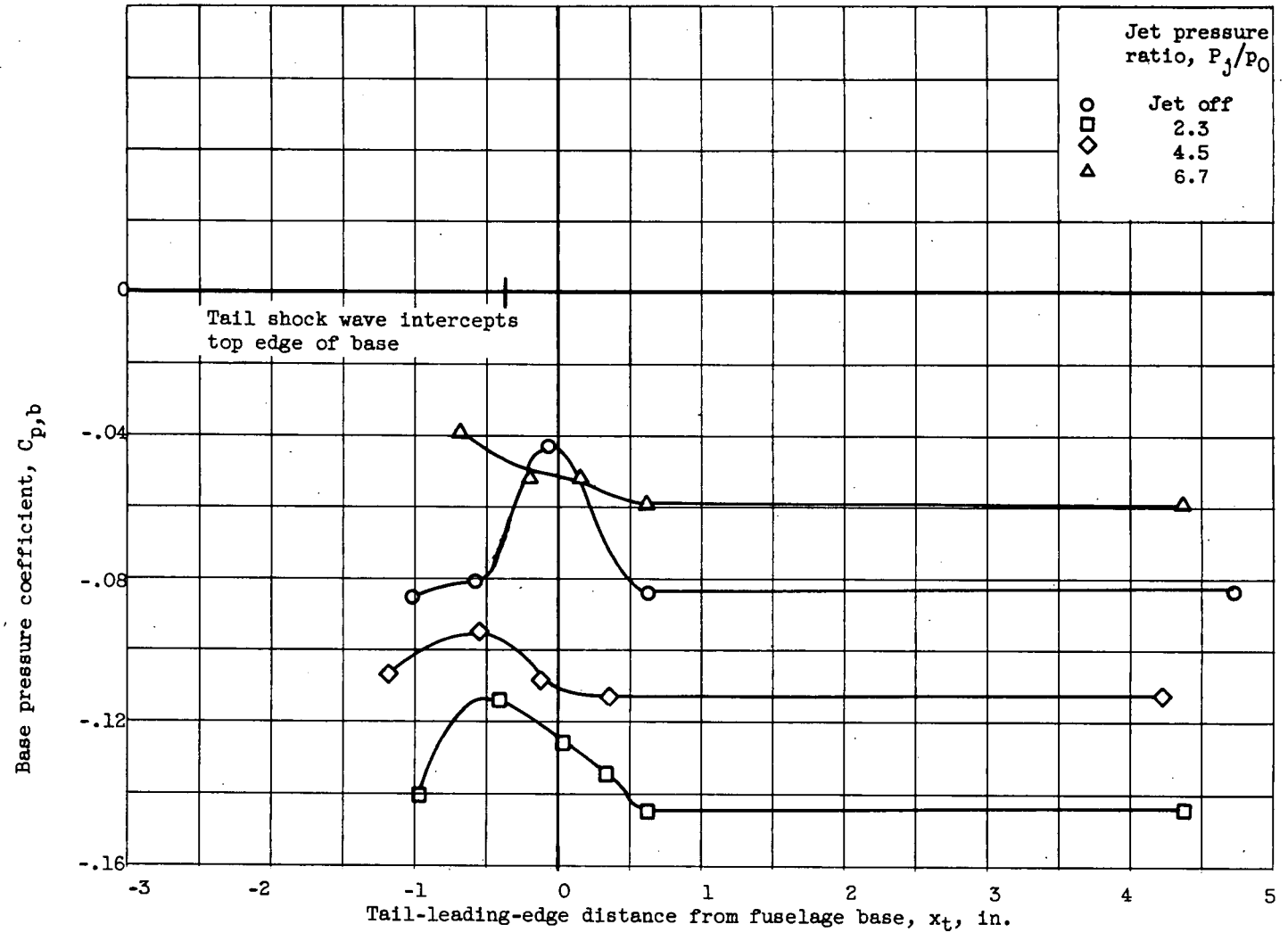


(b) Distance from fuselage centerline, 0.86 inch.

Figure 12. - Continued. Effect of tail shock wave on base pressure coefficient.

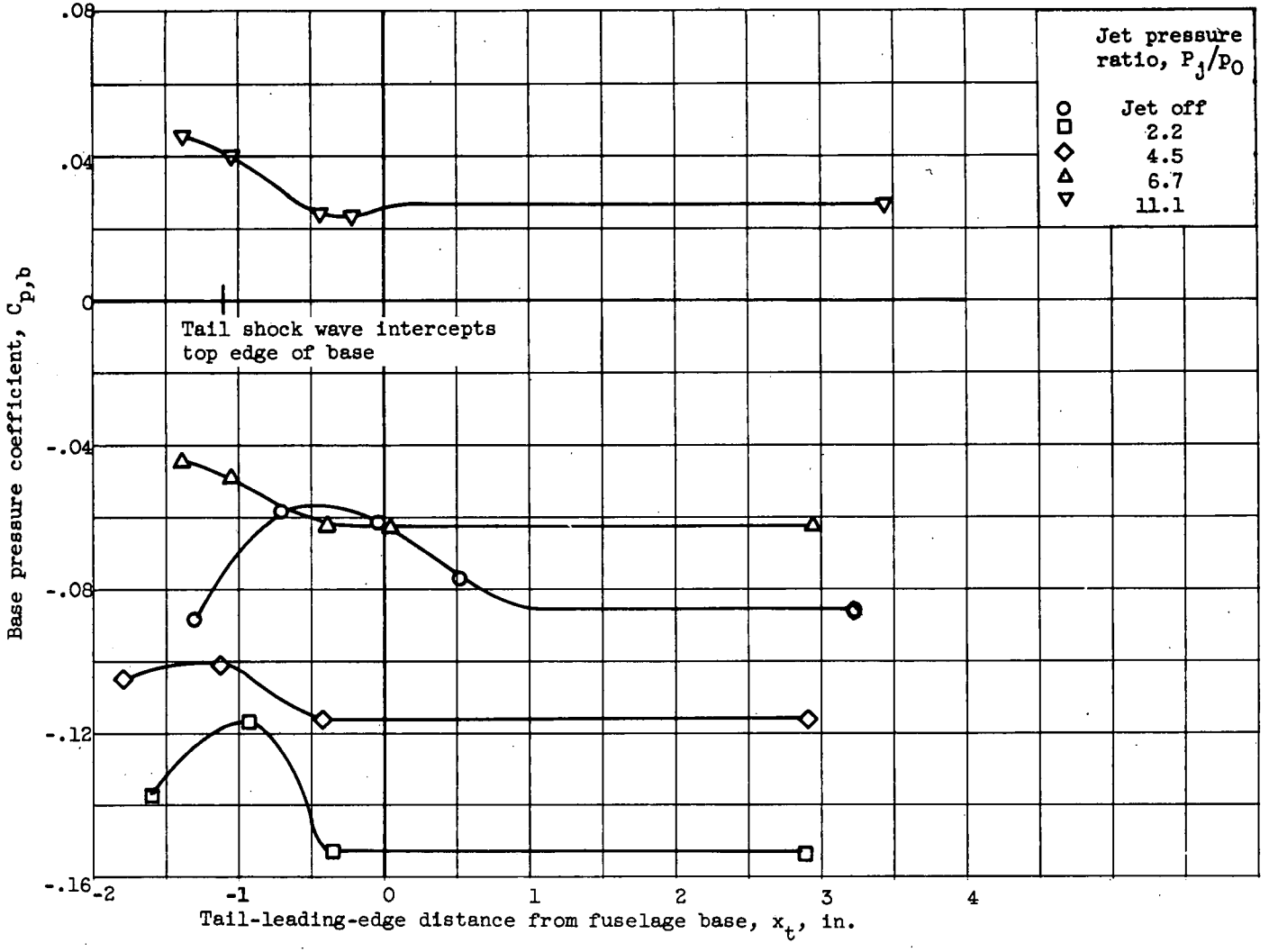


(c) Distance from fuselage centerline, 1.35 inches.

Figure 12. - Continued. Effect of tail shock wave on base pressure coefficient.

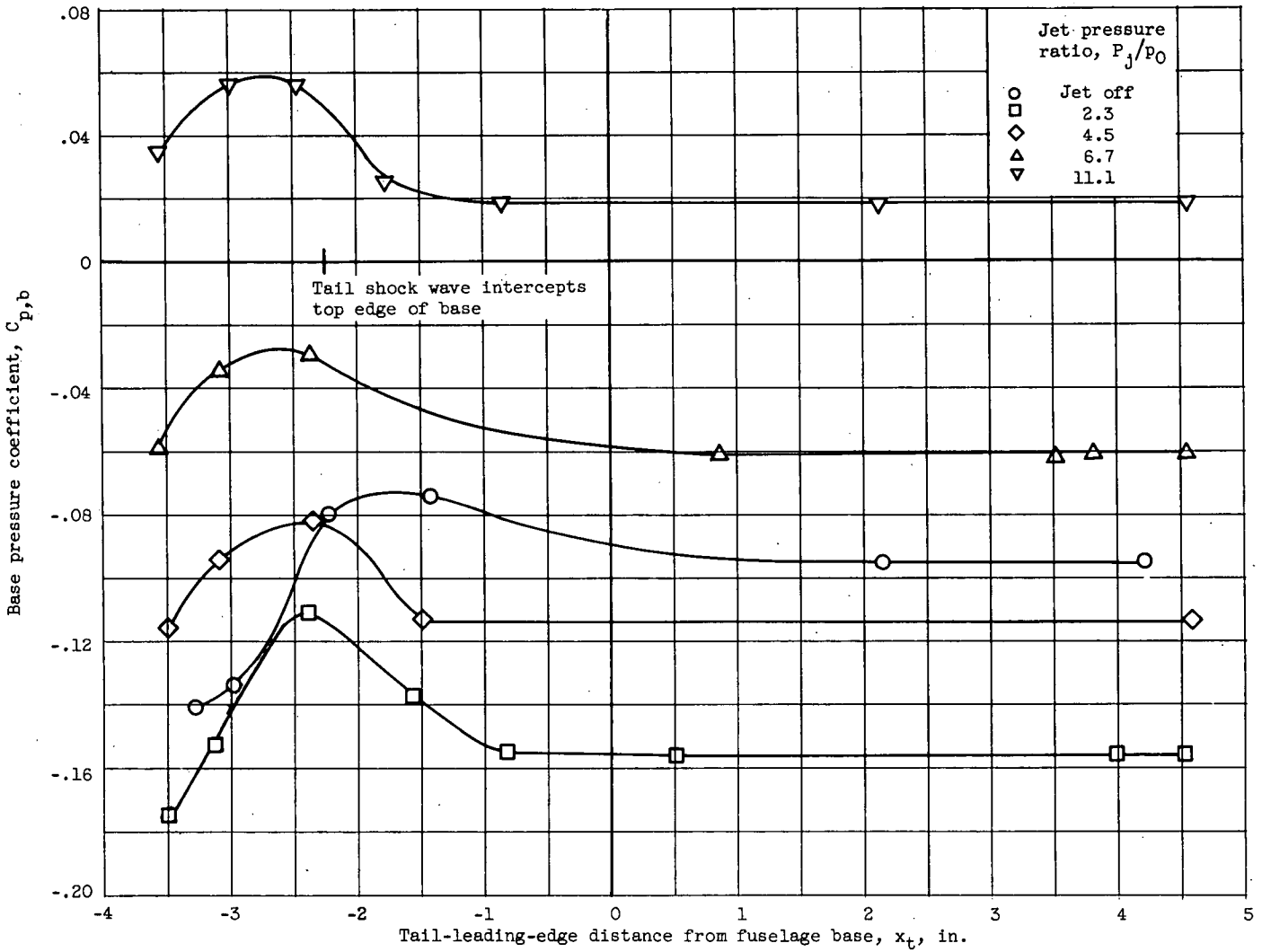


(d) Distance from fuselage centerline, 2.11 inches.

Figure 12. - Continued. Effect of tail shock wave on base pressure coefficient.

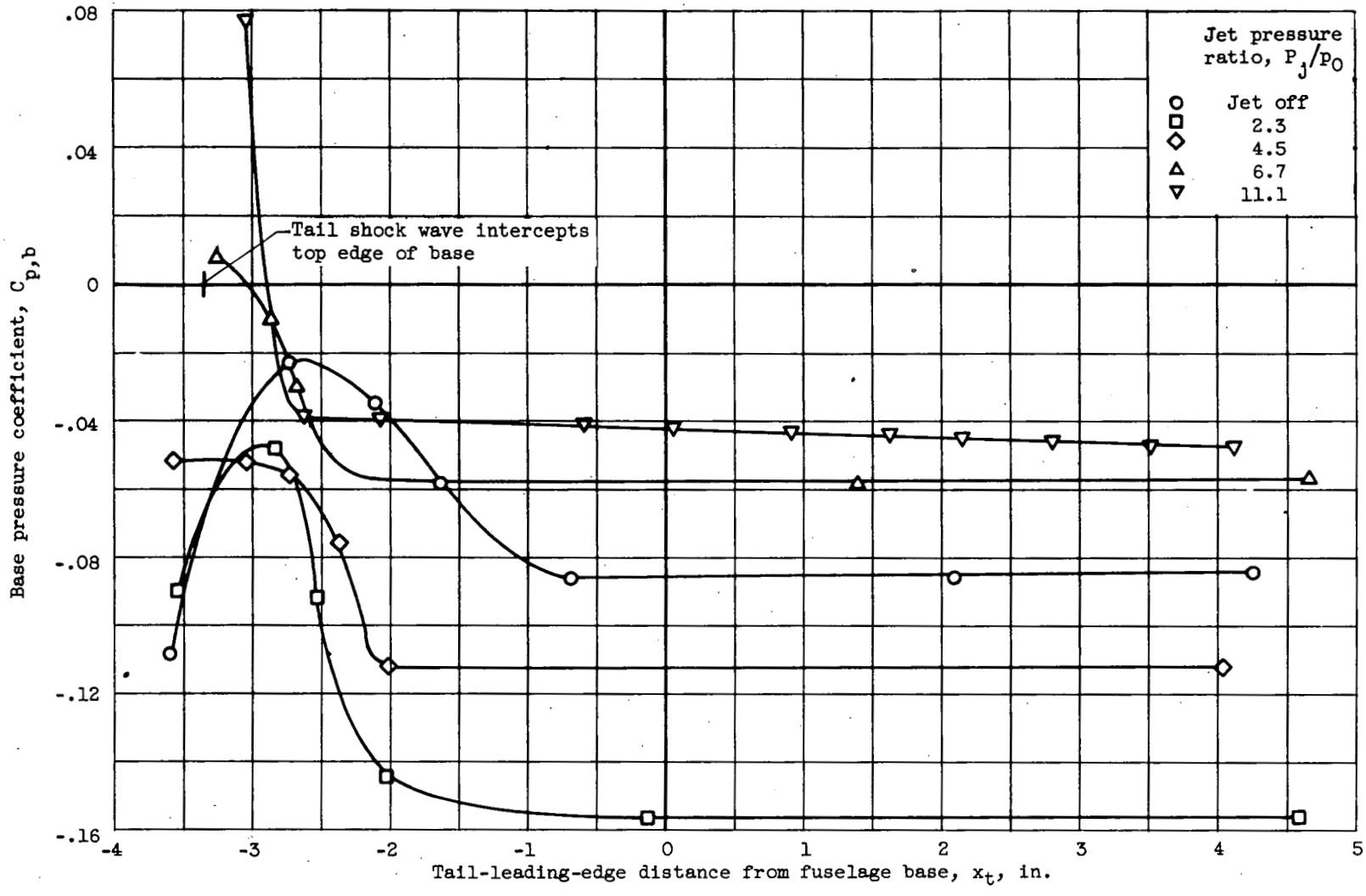


(e) Distance from fuselage centerline, 2.86 inches.

Figure 12. - Concluded. Effect of tail shock wave on base pressure coefficient.